ResearchGate

See discussions, stats, and author profiles for this publication at: https://www.researchgate.net/publication/260250327

Kizilcaören Ore-bearing Complex with Carbonatites (Northwestern Anatolia, Turkey): Formation Time and Mineralogy of Rocks

Article *in* Geology of Ore Deposits · February 2014

DOI: 10.1134/S107570151401005X

CITATIONS
30

READS
723

4 authors:



A. V. Nikiforov
Russian Academy of Sciences
52 PUBLICATIONS **502** CITATIONS
SEE PROFILE



Hüseyin Öztürk
İstanbul University-Cerrahpaşa
45 PUBLICATIONS **396** CITATIONS
SEE PROFILE



Sinan Altuncu
Ömer Halisdemir University
11 PUBLICATIONS **67** CITATIONS
SEE PROFILE



V. A. Lebedev
Russian Academy of Sciences
260 PUBLICATIONS **1,881** CITATIONS
SEE PROFILE

Some of the authors of this publication are also working on these related projects:

The revealing of geochemical evolution, P-T conditions and mantle sources for continental alkaline magmatism in the transition zone from intraplate to collision geotectonic setting (example of Eastern Anatolia and the northernmost of Arabian Plate) View project

Program of basic research of the Presidium of Russian Academy of Sciences #15 "The natural catastrophes and adaptive processes under the conditions of climate changing and development of nuclear power engineering". View project

All content following this page was uploaded by V. A. Lebedev on 20 February 2014.

The user has requested enhancement of the downloaded file.

ISSN 1075-7015, Geology of Ore Deposits, 2014, Vol. 56, No. 1, pp. 35–60. © Pleiades Publishing, Ltd., 2014.
Original Russian Text © A.V. Nikiforov, H. Öztürk, S. Altuncu, V.A. Lebedev, 2014, published in Geologiya Rudnykh Mestorozhdenii, 2014, Vol. 56, No. 1, pp. 41–69.

Kizilcaören Ore-bearing Complex with Carbonatites (Northwestern Anatolia, Turkey): Formation Time and Mineralogy of Rocks

A. V. Nikiforov[a], H. Öztürk[b], S. Altuncu[c], and V. A. Lebedev[a]

[a] *Institute of Geology of Ore Deposits, Petrography, Mineralogy, and Geochemistry, Russian Academy of Sciences, Staromonetnyi per. 35, Moscow, 119017 Russia*

[b] *Istanbul University, Department of Geological Engineering, Avcilar Campus, Istambul, Turkey*

[c] *Nigde University, Department of Geological Engineering, Nigde, Turkey*

Received June 8, 2012

Abstract—The results of isotope-geochronological and mineralogical studies of the rocks making up the Kizilcaören fluorite–barite–REE deposit, northwestern Anatolia, Turkey are discussed in the paper. The ore is a constituent of the subvolcanic complex localized in a large fault zone. The complex combines (from earlier to later rocks): (1) phonolite and trachyte stocks, (2) carbonatite and carbonate–silicate dikelike bodies; and (3) fluorite–barite–bastnaesite ore in the form of thick homogeneous veins and cement in breccia. The K–Ar dating of silicate igneous rocks and carbonatites shows that they were formed in the Chattian Age of the Oligocene 25–24 Ma ago. Mineralogical observations show that the ore is the youngest constituent in the rock complex. Supergene alteration deeply transformed ore-bearing rocks, in particular, resulting in leaching of primary minerals, presumably Ca–Mn–Fe carbonates, and in cementation of the residual bastnaesite–fluorite framework by Fe and Mn hydroxides. Most of the studied rocks contain pyrochlore, LREE fluorocarbonates, Nb-bearing rutile, Fe–Mg micas, and K-feldspar. The genetic features of the deposit have been considered. In general, the ore-bearing rock complex is compared in the set of rocks and their mineralogy and geochemistry with deposits of the Gallinas Mountains in the United States, the Arshan and Khalyuta deposits in the western Transbaikalia region, and Mushugai-Khuduk deposit in Mongolia. The Kizilcaören deposit represents a variant of postmagmatic mineralization closely related to carbonatite magmatism associated with alkaline and subalkaline intermediate rocks.

DOI: 10.1134/S107570151401005X

INTRODUCTION

More than half of the world's LREE resources are currently related to carbonatite massifs; however, economic LREE deposits are extremely rare among a wide range of carbonatite-bearing complexes primarily occurring at ancient platforms. The Kizilcaören fluorite–barite–LREE deposit is a unique example of ore-bearing carbonatites occurring out of Precambrian cratons.

The deposit was discovered in 1959 and then studied by Delaloye and Özgenç (1983), Stumpf and Kırıkoğlu (1986), Özgenç (1993), Hatzl and Morteani (1993), and Gültekin et al. (2003). The ore is represented by bastnaesite–barite–fluorite mineral aggregate in veins and mineralized breccia traced to a depth of 200 m. According to Gültekin et al. (2003), the reserves of this deposit are (Mt): 4, LREE (Ce, La, Nd); 0.4, ThO_2; 10, fluorite, and 40, barite. Phonolite, trachyte, and carbonatite are associated with orebodies.

Despite the relatively detailed study of the deposit, its origin remains ambiguous, because most studies focused on the structure of orebodies and their formation conditions. Inferences on links of mineralization to alkaline igneous rocks and carbonatites remain insufficiently substantiated and primarily rely on joint occurrence of various rocks at the deposit. A geological approach to solving this problem is inefficient, because the contacts between orebodies, on the one hand, and phonolite and carbonatite, on the other, have not been observed. Mineralogical data, in particular, recognition of index minerals contained in various rocks, are also equivocal, because the chemical compositions of the minerals have not been reported. Mineralogy of carbonatites remains unstudied as well. More or less sufficient information available for phonolites (Santfakıoğlu et al., 2009) has not been compared with that for carbonatite and ore. Geochronological evidence has not ascertained the situation. The study was carried out in the 1980s and used an imperfect technique of whole-rock sample dating using the K–Ar method (Delaloye and Özgenç, 1983). The age estimates of carbonatite (29 ± 1 Ma) and phonolite (23 ± 1 Ma) practically ruled out their joint formation. Nevertheless, the association of alkaline rocks, carbonatite, and fluorite–barite–LREE ore at similar deposits elsewhere stimulated the search for evidence of their cognation.

Corresponding author: A.V. Nikiforov. E-mail: nikav@igem.ru

Table 1. Geographic coordinates (degrees, WGS 84 coordinate system) of the studied rock samples taken from Kizilcaören deposit

Rock type	Sample number (latitude/longitude)
Phonolite	382 (39.59004/31.34031); 384 (39.59395/31.32950)
Trachyte breccia with barite–fluorite cement	374 (39.60569/31.37034)
Phlogopite–calcite–albite rock	360 (39.60747/31.36096)
Phlogopite–calcite carbonatite	362-b (39.59486/31.35635)
Fluorite–barite–bastnaesite ore	361 (39.59673/31.35563); 362 (39.59488/31.35551);
	364 (39.60007/31.37547); 366 (39.59973/31.37616);
	367 (39.60091/31.37495); 370 (39.60051/31.37366);
	375 (39.60634/31.36923); 378 (39.61223/31.37457);
	379 (39.60382/31.35283); 380 (39.60293/31.35327).

In this paper, we discuss the chronological and genetic alliance of igneous rocks and ore at the deposit based on a K–Ar geochronological study carried out with allowance for up-to-date methodical requirements. Close scrutiny of the minerals contained in rocks allowed us to find evidence for their genetic links.

GEOLOGY OF THE COMPLEX

The Kizilcaören Complex occurs in the Tavşanli Zone (Fig. 1, inset), which is a constituent of the Anatolian Terrane and corresponds to the northern paleosubduction zone of the young Anatolian Platform (Okay et al., 1998; Sherlock et al., 1999, Moix et al., 2008).

The rocks are localized near a large structural suture that separates serpentinized ultramafic rocks of the Permian–Triassic island-arc complex from the Late Paleozoic–Triassic accretionary complex (sandstone, graywacke, phyllite, basic rocks).

The geological scheme (Fig. 1) has been compiled on the basis of published data (Özgenç, 1993; Gültekin et al., 2003; Santfakıoğlu et al., 2009) and the authors' observations. Geographic coordinates of the samples are given in Table 1.

The Kizilcaören Complex comprises phonolite and trachyte stocks, sporadic dike-shaped bodies of carbonatites and carbonate–silicate rocks, and stockwork zones of bastnaesite–barite–fluorite ore. The mineral composition of the main rocks is shown in Fig. 2).

Alkaline silicate rocks occur to the north of the structural suture (Fig. 1). Three stocks about 500 m in diameter are clearly expressed in the topography against country serpentinized ultramafic rocks. Two of the sampled stocks are composed of phonolites that have crystallized to various degrees. The third stock consists of trachyte (Santfakıoğlu et al., 2009). Trachytic tuffs are noted in western part of the complex (Özgenç, 1993; Gültekin et al., 2003).

Carbonatites and carbonate–silicate rocks make up irregularly shaped bodies within zones of tectonic breccia. According to Özgenç (1993), carbonatites occur as veins 1.0–1.5 m thick, which like the orebodies are hosted in terrigenous rocks of the accretionary complex. Only one carbonatite vein is known in ultramafic rocks pertaining to the island-arc complex.

The ore at the Kizilcaören deposit is composed of porous medium- to coarse-grained bastnaesite–barite–fluorite aggregate, which fills thick (a few meters) and extended (tens and hundreds of meters) veins localized in crush zones or cements tectonic and volcanic (?) breccia. The veined and stockwork orebodies are distinguished, correspondingly.

The ore veins are characterized by banding oriented conformably to the strike of veins and contain fragments of country rocks. The number of fragments increases in the contact zone, where the banded ore grades into breccia cemented by ore material. The mineralized breccia is also localized independently of ore veins. Özgenç (1993) described large (more than 500 m) eruptive explosion pipes cemented by ore.

Widespread and intense supergene leaching and cementation markedly affected texture–structural features of ore and its mineralogy. Signs of leaching are seen almost overall in porous, cavernous, and poorly cemented ore varieties. The leached cavities are filled with Fe and Mn hydroxides, which also occur as massive sinters.

AGE OF ROCKS

The isotope-geochronological study of igneous rocks at the Kizilcaören deposit was carried out using the K–Ar method at the Laboratory of Isotope-Geochemistry and Geochronology of the Institute of Geology of Ore Deposits, Petrography, Mineralogy, and Geochemistry, Russian Academy of Sciences. Phonolite (samples 382, 384), carbonate–silicate rock, and carbonatite (samples 360, 362-b) have been dated (Table 2). Unfortu-

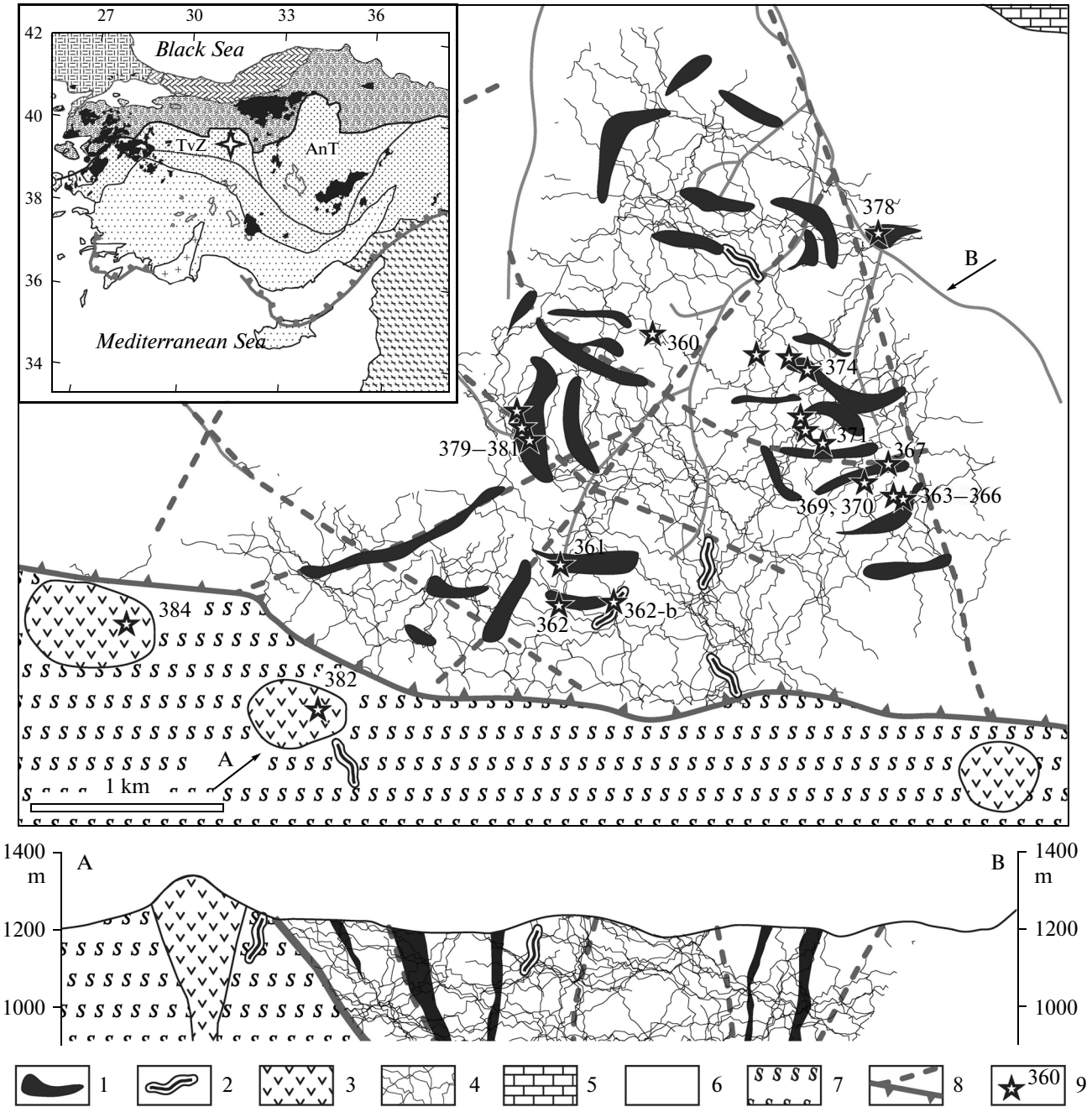


Fig. 1. Geology of the Kizilcaören fluorite–barite LREE deposit and its regional tectonic position (inset), after Özgenı (1993), Gültekin et al. (2003), and Santfakıoğlu et al. (2009). (1) Oligocene ore veins and breccias with ore-bearing cement; (2) Oligocene carbonatite; (3) Oligocene phonolite and trachyte; (4) brecciated rocks; (5) Permian limestone; (6) Triassic metaarkose, metagraywacke, phyllite, and dolerite; (7) Triassic serpentinite; (8) fault zones mapped and inferred; (9) location of sample and its number. Location of Kizilcaören deposit in inset is indicated by star. Tectonic blocks are shown after Moix et al. (2008), including Anatolian Terrane (AnT) and Tavşanli Zone (TvZ). Early and middle Miocene volcanic fields are shown in black, after geological maps on a scale of 1 : 500 000, General Directorate of Mineral Research and Exploration, Ankara, Turkey.

nately, the K-bearing phases (phlogopite, K-feldspar) have been altered to a degree unfit for dating.

The concentrations of radiogenic argon were determined on a MI-1201 IG mass spectrometer (SELMI, Ukraine) using the isotope dilution method with the ^{38}Ar as spike. The K contents were determined with flame spectrophotometry on an FPA-01 device (Elam-Center, Russia). The commonly adopted decay constant of K (Steiger and Jager, 1977) was used for age calculation.

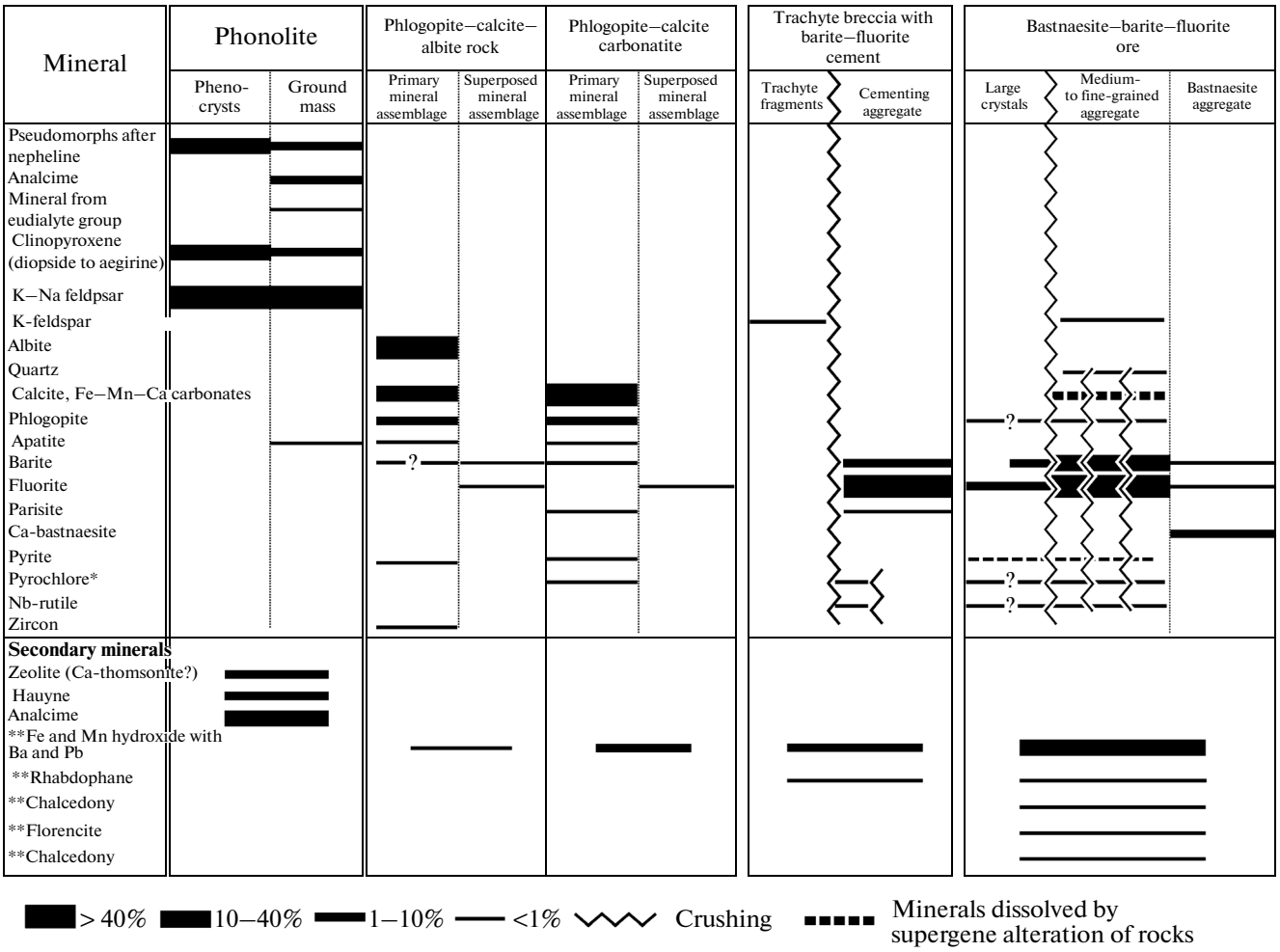


Fig. 2. Mineralogy of rocks belonging to the Kizilcaören Complex. *Pyrochlore altered by supergene processes; **supergene minerals.

The groundmass of phonolite free of phenocrysts was used for dating to avoid overestimation of isotopic age due to possible excess ^{40}Ar in phenocrysts (Fig. 2). Our dates (24.1 ± 0.6 and 24.8 ± 0.6 Ma) coincide with each other within the limits of analytical uncertainty and agree with the earlier published series of isotopic dates (24.20 ± 0.08, 24.53 ± 0.11, 24.58 ± 0.08, 24.35 ± 0.12) obtained by the Ar/Ar method for sanidine phenocrysts from phonolite (Santfakıoğlu et al., 2009). The average of two new and four earlier published dates yields 24.4 ± 0.5 Ma. Thus, the age of phonolite corresponds to the Chattian (Late Oligocene).

The K–Ar age of carbonate–silicate rock and carbonatite was determined using fractions of packet-type phlogopite crystals scattered throughout these rocks (Table 2). The K–Ar dates (25.7 ± 0.6 and 24.9 ± 0.6) coincide with each other within the limits of analytical uncertainty; however, differ significantly from the estimates obtained for whole-rock samples (28.7 ± 1.0 Ma) by Delaloye and Özgenç (1983). Our data show that phonolite, on the one hand, and carbonate–silicate rock and carbonatite, on the other, are practically coeval. This implies that the entire series of the studied rocks from the Kizilcaören deposit formed almost synchronously 24–25 Ma ago.

As was mentioned above, the ore remains directly undated; however, one can judge the age of ore-bearing bastnaesite–fluorite–barite rock from the results of mineralogical observations. In our opinion, the superposed fluorite mineralization that occurs in carbonatite was formed contemporaneously with ore deposition. It is our guess that the ore is only slightly younger in age than the igneous rocks exposed at the deposit.

Late Oligocene magmatic events are infrequent in central and western Turkey. Volcanic rocks of this age are known in northwestern Turkey (Ercan et al., 1985; Ercan and Satir, 1994), where they are related to initial stage of the vigorous early–middle Miocene magmatic pulse (Fig. 1, inset) characterized by eruptions of calc-alkaline andesites and rhyolites. High-K calc-alkaline shoshonites are also widespread (Dilek and

Table 2. K–Ar age of phlogopite–calcite–albite rock (sample 360), phlogopite–calcite carbonatite (sample 362b), and phonolites (samples 382, 384) from Kizilcaören deposit

Sample	Material	Potassium, wt % ± σ	$^{40}Ar_{rad}$, ng/g ± σ	Age, Ma ± 2σ
360	Phlogopite	7.88 ± 0.08	14.16 ± 0.07	25.7 ± 0.6
362-b	"	8.88 ± 0.09	15.43 ± 0.06	24.9 ± 0.5
382	Groundmass	4.18 ± 0.05	7.05 ± 0.02	24.1 ± 0.6
384	"	4.46 ± 0.05	7.73 ± 0.03	24.8 ± 0.6

Altunkaynak, 2009, 2010). Phonolites as alkaline rocks proper are known only in the Kizilcaören Complex.

ORE-BEARING MAGMATISM

Alkaline Silicate Rocks

The alkaline magmatism at the deposit and nearby is represented by phonolite stocks. The rock is characterized by porphyritic structure (Fig. 3a). The phenocrysts occupying 30–40% of rock volume are elongated (up to 10 mm) tabular alkali feldspar crystals (40–60%), pyroxene crystals (20–30%), and pseudomorphs of secondary minerals after nepheline (20–30%). The groundmass (0.01–0.50 mm) has an allotriomorphic-granular (agpaitic) structure and consists of alkali feldspar microlites (55–65 vol %), pseudomorphs of late minerals after nepheline (10 vol %), analcime (up to 20 vol %), pyroxene (10 vol %), and an unidentified mineral from the eudialyte group (<1 vol %) (Fig. 2). The average (of two samples) chemical composition of phonolite is as follows (wt %): 57.6 SiO_2, 0.25 TiO_2, 19.3 Al_2O_3, 3.15 $(Fe_2O_3)_{tot}$, 0.18 MnO, 0.70 MgO, 1.9 CaO, 7.50 Na_2O, 5.44 K_2O, 0.04 P_2O_5, 3.5 LOI, 0.16 Ba, 0.11 Sr, and 0.11 Zr.

Alkali feldspar contains Ba, Fe, Mg, and Ca as admixtures (Table 3) and is characterized by variable proportions of orthoclase and albite end members (39–81% Or). This variation is retained among microlites in the groundmass and larger crystals, including phenocrysts. The composition of microlites covers the entire aforementioned range. The phenocryst compositions are more stable, and the outer zones are enriched in K. In addition, the zoning of alkali feldspar crystals is expressed in the variation of Ba contents. The crystal core, as a rule, is enriched in Ba with gradual transition to the outer zone with a lower Ba content. In rare cases, large phenocrysts consist of three zones: the inner and outermost zones are depleted in Ba, whereas the intermediate zone is enriched in celsian end member.

Pyroxene phenocrysts (more than 1 mm in size) and microlites differ in composition (Table 4). In medium-grained phonolite (sample 382), yellowish green pyroxene phenocrysts are composed of diopside rimmed by green aegirine-augite with K-feldspar and nepheline inclusions. In fine-grained phonolite (sample 384), phenocrysts are completely composed of aegirine-augite. In the groundmass of both phonolite varieties pyroxene is dominated by aegirine end member and also enriched in small K-feldspar inclusions. Santfakıoğlu et al. (2009) noted no diopside in phonolite. Aegirine-augite was identified in phenocryst cores and aegirine in the outer rim. This implies that the equilibrium pyroxene composition evolved in the course of melt evolution in the sequence diopside → aegirine-augite → aegirine.

A euhedral mineral with hexagonal and rectangle sections of a hexagonal prism in plane of a thin section (Fig. 3a) is widespread among phenocrysts. This is most likely nepheline, which has been completely replaced with aggregate of secondary minerals. Nepheline was identified as unaltered inclusions up to 10 μm in size incorporated into pyroxene. The chemical composition of nepheline is presented in Table 5. All pseudomorphs are enriched in submicrometric black inclusions; in one case, Ba and Sr sulfate has been identified.

In fine-grained phonolite, pseudomorphs are composed of a mineral from sodalite group close to hauyne in chemical composition (Table 5).

In coarser-grained phonolite, the overwhelming majority of pseudomorphs consist of zeolite close to Ca-thomsonite in composition (Table 6). Sporadic euhedral hauyne pseudomorphs occur in the groundmass of this rock. Hauyne was also detected as a 50-μm inclusion in K-feldspar crystal.

Analcime is another mineral that forms pseudomorphs after nepheline (Table 6). In addition to pseudomorphs, analcime frequently fills xenomorphic interstices between other minerals and occurs as cross-cutting veinlets.

A yellow unidentified mineral from the eudialyte group was found in relatively coarse-grained phonolite, where it occurs in the groundmass as isolated crystals or aggregates in intergrowths with feldspar, analcime, and nepheline replaced with zeolite (Fig. 3b). The crystals of this mineral are 50–200 μm in size. They are commonly anhedral; however, hexagonal sections are noted as well. The chemical composition (Table 7) is

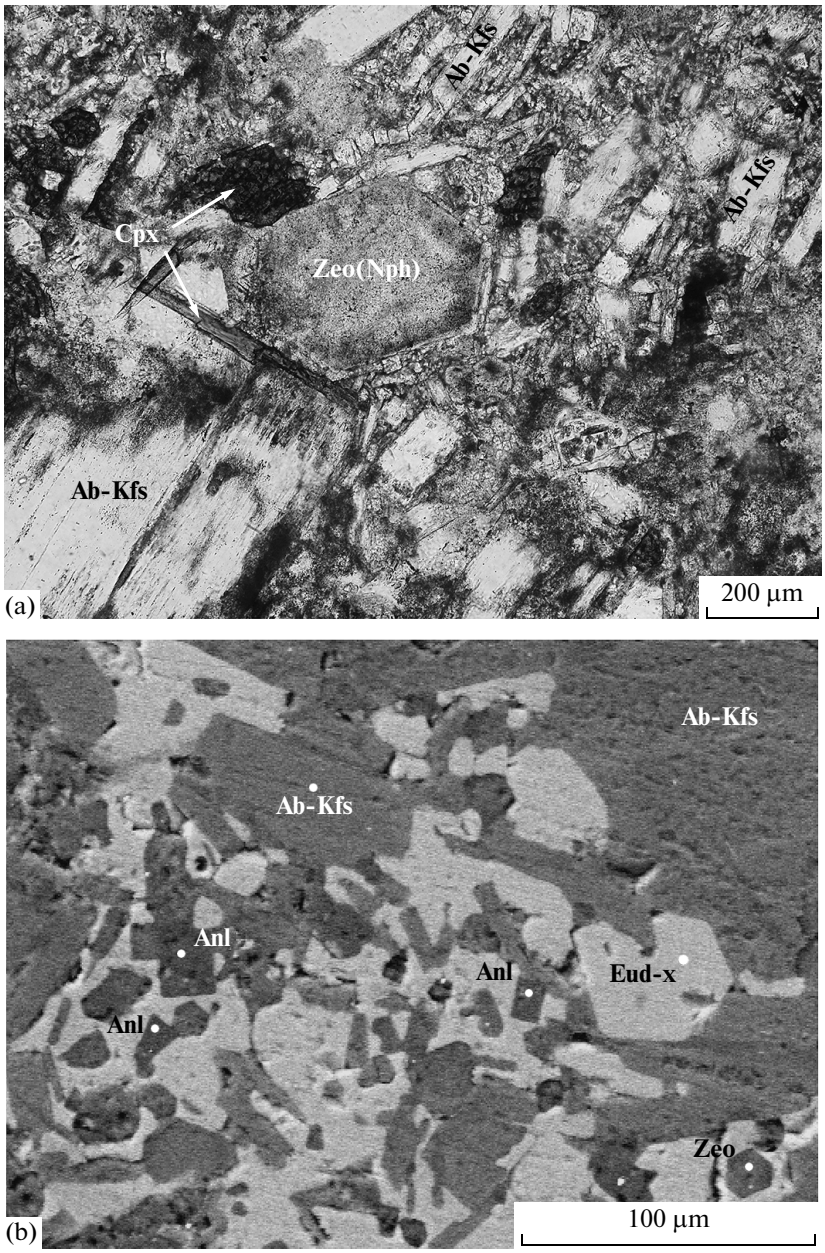


Fig. 3. Photomicrographs of phonolite (sample 382): (a) thin section in transmitted light; (b) SEM image in reflected electrons. Here and hereafter: Ab, albite; Ab-Kfs, K–Na feldspar; Anl, analcime; Ap, apatite; Brt, barite; Bst, Ca-bastnaesite; Cal, calcite; Cpx, clinopyroxene; Eud-x, unidentified mineral from eudialyte group; Hyn, hauyne; Fl, fluorite; Flg, Fe–Mg mica; Kfs, K-feldspar; Nph, nepheline; Oxd, Fe–Mn hydroxide; Par, parisite; Pcl, pyrochlore; Phl, Fe–Mg mica of annite–phlogopite or siderophyllite–eastonite series; Rbd, rhabdophane; Zeo, zeolite; Zrn, zircon.

readily recalculated to the eudialyte metrics with extremely low Na and K contents. The main part of alkali-metal site A is probably occupied by H_2O. This makes this mineral close to aqualite, a member of the eudialyte group; however, as judged from the calculation results, we are dealing with a new mineral more enriched in water.

Apatite, which occurs in phonolite in accessory amounts, is occasionally incorporated into pyroxene. Pyrite, galena, and REE-bearing fluorocarbonate a few micrometers in size were identified in the groundmass of phonolite.

Carbonatites and Carbonate–Silicate Rocks

Carbonatite dikes occur at the deposit in spatial association with ore. We have sampled phlogopite–calcite (sample 362b) and phlogopite–calcite–albite (sample 360) rocks with superposed fluorite mineralization (Fig. 2) indicating that ore formation followed

Table 3. Chemical composition of alkali feldspar and nepheline from phonolite, wt %

Component	Medium-grained phonolite, sample 382						Fine-grained phonolite, sample 384				
	382_27*	382(14)	382(13)	382(25)	382(19)	382(20)	384(29)	384_9*	384_10*	384(27)	384(28)
	GM-micro	*GM-micro*	*GM-micro*	*GM-micro*	*PH*	*PH*	*GM-micro*	*PH*	*PH-r*	*PH*	*PH-r*
SiO_2	65.31	63.49	62.1	61.2	63.29	63.88	62.58	61.45	62.74	59.05	60.7
Al_2O_3	18.61	20.86	19.88	19.94	20.69	20.01	19.18	18.93	19.36	22.16	21.51
MgO	–	–	1.07	–	–	–	1.01	–	–	–	–
CaO	0.12	–	0.81	–	–	–	–	0.04	0.08	–	–
BaO	0.16	–	–	–	–	–	–	1.7	0.16	4.43	3.7
Fe_2O_3	0.38	–	0.53	–	–	0.54	0.61	0.59	0.79	–	–
Na_2O	7.11	6.97	5.2	2.23	5.16	5.5	4.46	4.82	6.66	4.21	3.97
K_2O	6.88	7.89	8.99	14.22	9.51	9.13	9.86	8.86	7.51	8.91	9.51
Total	98.57	99.21	98.58	97.59	98.65	99.06	97.7	96.39	97.3	98.76	99.39
An	*0.6*	*0*	*3.9*	*0*	*0*	*0*	*0*	*0*	*0*	*0*	*0*
Ab	*60.7*	*57.3*	*45.0*	*19.2*	*45.2*	*47.8*	*40.7*	*45.1*	*57.2*	*41.8*	*38.8*
Or	*38.7*	*42.7*	*51.2*	*80.8*	*54.8*	*52.2*	*59.3*	*54.7*	*42.5*	*58.2*	*61.2*

GM-micro, microlite in groundmass; PH, phenocryst and core of large (>1 mm) phenocryst; PH-r rim of large phenocryst. From here on, chemical compositions of minerals determined on JSM-5610LV SEM equipped with Oxford INCA 250 EDS at Institute of Geology of Ore Deposits, Petrography, Mineralogy, and Geochemistry, Russian Academy of Sciences (IREM RAS). Dash denotes below detection limit; *on a JXA 8200 microprobe (IGEM RAS).

Table 4. Chemical composition of clinopyroxene from phonolite, wt %

Component	382(11)	382(12)	382_23*	382_24*	384_8*	384_12*	382(16)	382(9)	382_18*	384-32	384_4*	384_6*	**	**
	PH	RF	PH	RF	PH	PH	GM-micro	GM-micro	GM-micro	GM-micro	GM-micro	GM-micro	PH	RF
SiO_2	47.06	47.24	50.68	52.02	49.35	51.57	52.79	52.19	51.98	54.17	51.18	51.43	50.57	52.41
TiO_2	0.86	2.39	0.17	0.34	0.76	0.45	0.63	0.96	0.5	0.63	1.19	0.57	0.29	1.92
Al_2O_3	6.52	0	2.24	0.72	1.86	0.86	1.19	1.2	0.52	–	0.73	0.75	1.17	0.72
Cr_2O_3	–	–	–	–	–	–	–	–	–	–	–	–	0.01	0.05
FeO	11.63	29.08	13.46	27.28	19.31	23.37	30.11	23.42	27.55	26.88	23.55	23.54	23.76	29.99
MnO	–	–	0.33	0.45	1.15	0.81	–	–	0.75	–	0.86	0.78	0.89	0.39
MgO	10.36	–	9.38	0.84	4.66	2.67	0.96	3.88	0.66	2.47	2.28	2.28	2.92	0.5
CaO	21.7	14.7	22.31	4.5	17.26	9.52	4.15	11.15	4.89	8.43	8.97	9.7	13.38	2.22
Na_2O	1.24	6.75	1.07	11.65	3.93	8.51	10.54	8.14	11.71	9.91	8.68	8.67	6.79	12.42
Total	99.37	100.16	99.64	97.8	98.28	97.76	100.37	100.94	98.56	102.49	97.44	97.72	99.78	100.62
Jd	*8.15*	*0.00*	*5.52*	*10.53*	*5.57*	*11.50*	*16.20*	*6.82*	*8.03*	*9.25*	*14.48*	*11.22*	*2.50*	*13.65*
Ac	*0.98*	*50.64*	*2.47*	*75.40*	*24.59*	*51.61*	*59.80*	*51.99*	*78.02*	*60.42*	*49.01*	*53.03*	*48.78*	*73.38*
Aug	*90.87*	*49.36*	*92.01*	*14.07*	*69.84*	*36.89*	*24.00*	*41.19*	*13.95*	*30.33*	*36.50*	*35.75*	*48.72*	*12.97*

* See notes to Table 3.

** Sanfakioğlu E., *J. Asian Earth Sci.*, 2009, vol. 35. GM-micro, microlite in groundmass; PH, core and PH-r rim of phenocryst.

crystallization of carbonatites and carbonate-bearing rocks.

Phlogopite–calcite carbonatite is a greenish brown medium-grained banded rock consisting of calcite (>90 vol %), phlogopite (5 vol %), barite (1 vol %), apatite (<1 %) and pseudomorphs of Fe and Mn hydroxides after pyrite (?). Pyrochlore and parisite occur in accessory amounts.

Table 5. Chemical composition of hauyne and nepheline from phonolite, wt %

Component	Hauyne								Nepheline	
	382(17)	382(22)**	382(21)**	384(31)	384(33)	384_3*	384_5*	384_7*	382_25*	382_26*
SiO_2	38.28	36.39	34.54	41.15	42.42	43.25	42.95	42.88	45.54	46.02
Al_2O_3	32.35	30.95	28.16	30.36	31.27	30.51	30.5	30.23	31.04	31.4
CaO	3.44	1.38	1.99	3.17	2.52	0.74	2.9	3.23	0.02	0.01
SrO	–	–	2.23	–	–	–	–	–	–	–
BaO	–	–	2.69	–	–	0.03	0.06	0.004	–	–
FeO	0.7	–	–	0.43	–	0.25	0.32	0.33	1.71	1.52
Na_2O	16.17	16.73	16.64	12.23	13.06	13.33	11.44	11.29	17.49	17.18
K_2O	2.73	4.86	3.0	3.14	3.52	3.5	2.44	2.37	4.06	4.47
SO_3	6.01	7.59	9.11	6.19	5.72	6.61	6.19	6.42	–	–
Cl	–	–	–	–	–	0.04	0.08	0.11	–	–
Total	99.68	97.9	98.36	96.67	98.51	98.26	96.88	96.86	99.86	100.6

* See notes to Table 3.

** Analyses of sites in hauyne crystals with microinclusions of Ba–Sr sulfate, fractions of a micrometer in size: 382(22), site without inclusions; 382(21) site with inclusions.

Table 6. Chemical composition of analcime and zeolites from phonolite, wt %

Component	Analcime									Pseudomorphs of zeolite (Ca-thomsonite)					
	382(23)	382(26)	382(4)	382(24)	382(8)	384(30)	382_21*	382_22*	382(15)	382(2)	382(3)	382(12)	382_16*	382_17*	382_29*
SiO_2	54.32	55.49	53.06	51.90	53.10	54.87	54.94	58.54	36.05	38.36	40.93	38.13	45.3	39.34	41.16
Al_2O_3	23.98	25.29	24.21	24.41	24.27	24.62	25.47	23.84	30.88	28.01	34.29	32.12	24.95	30.23	29.42
CaO	–	–	0.93	–	–	–	0.97	0.09	12.83	11.1	13.24	13.35	11.55	12.26	12.03
FeO	0.41	–	–	–	0.33	–	0.23	0.23	–	–	–	–	0.05	0.03	0.13
Na_2O	10.11	11.49	10.57	13.85	12.11	10.77	11.69	10.67	3.13	4.66	3.4	3.29	2.98	3.76	1.23
K_2O	–	–	–	–	–	–	0.08	0.07	–	–	–	–	0.38	0.03	0.05
SO_3	–	–	–	–	–	–	0.08	0.02	–	–	–	–	0.24	0.06	0.14
Cl	–	–	–	–	–	–	1.14	0.19	–	–	–	–	0.03	0.01	0.05
Total	88.82	92.27	88.77	90.16	89.81	90.26	94.6	93.65	82.89	82.13	91.86	86.89	85.48	85.72	84.21

Calcite forms allotriomorphic-granular matrix with grain size lesser than 0.5 mm and contains a Mg admixture (<1 wt %). Small Fe and Mn hydroxide inclusions a few micrometers in size with admixtures of Si, Pb, and Ba are identified in calcite.

Phlogopite crystals are 0.5–0.7 mm in size are distributed uniformly or clustering in bands. The barrel-shaped apatite crystals are impregnated into calcite or accumulate within intergranular space. Barite with Sr admixture occur as separate grains 10 to 100 μm in size or their aggregates uniformly distributed through the rock. Parisite is identified as crystal intergrowths up to 20 μm in diameter or larger clusters of intergrowths (Fig. 4) filling interstices between calcite crystals. Euhedral pyrochlore crystals 10–20 μm are intergrown with calcite and identified within intergranular space of the calcite matrix (Fig. 4).

Fluorite and hydroxides variable in composition are superposed minerals. Fluorite occurs as amoeba-like granular aggregates light purple in color penetrating into intergranular space of the calcite matrix. Fe hydroxides replace pyrite, whereas Mn–Fe hydroxides with Pb and Ba admixtures fill interstices between major minerals.

Phlogopite–calcite–albite rock (sample 360) is a medium- to coarse-grained massive rock consisting of albite (65–75 vol %), calcite (20–25 vol %), phlogopite (5 vol %), and sporadic Fe hydroxide after pyrite. Barite, apatite, zircon, pyrochlore, and unidentified

Table 7. Chemical composition of mineral from eudialyte group in phonolite, wt %

Component	382(7)	382(11)	382_19*	382_30*	382_28*	382_41*	382_42*	382_43*
SO_3	–	–	0.07	0.04	0.04	0.02	0.04	0.01
Nb_2O_5	–	–	0.33	0.26	0.30	0.23	0.28	0.45
SiO_2	53.04	53.73	56.27	56.04	56.99	56.36	55.3	56.41
TiO_2	0.86	0.85	0.31	0.52	0.43	0.47	0.34	0.25
ZrO_2	10.57	11.65	13.77	11.96	13.56	13.41	13.17	13.57
Al_2O_3	–	–	0.24	0.65	0.11	0.12	0.08	0.1
CaO	11.99	11.34	11.87	11.16	11.75	11.7	11.71	11.84
MnO	0.83	0.74	1.13	1.12	1.14	0.9	0.84	1.11
FeO	2.83	3.32	2.95	3.24	3.05	2.98	3.23	2.92
BaO	–	–	–	0.14	0.11	0.11	0.002	0.07
Na_2O	3.04	3.05	2.8	3.45	2.52	2.21	2.92	2.75
K_2O	1.69	1.44	0.9	1.12	1.04	0.72	0.69	0.39
Cl	2.14	1.95	2.44	2.32	2.33	2.32	2.41	2.46
H_2Ocalc	7.38	7.49	8.11	8.00	8.36	8.51	8.00	8.31
Total	94.37	95.56	101.19	100.02	101.73	100.06	99.01	100.64

SO_3, Al_2O_3, and BaO contents were omitted in calculations.

382(7). $(11.21H_2O \cdot Na_{2.78}K_{1.02})_{15}Ca_{6.06}(Fe_{1.12}Mn_{0.33})_{1.45}(Zr_{2.43}Ti_{0.30})_{2.73}[Si_{25}(O_{64.01} \cdot 8.99H_2O]_{73} \cdot 3H_2O \cdot Cl_{1.71}$

382(11). $(11.39H_2O \cdot Na_{2.75}K_{0.85})_{15}Ca_{5.65}(Fe_{1.29}Mn_{0.29})_{1.58}(Zr_{2.64}Ti_{0.30})_{2.94}[Si_{25}(O_{64.15} \cdot 8.85H_2O]_{73} \cdot 3H_2O \cdot Cl_{1.54}$

382_19. $(12.08H_2O \cdot Na_{2.41}K_{0.51})_{15}Ca_{5.65}(Fe_{1.10}Mn_{0.43})_{1.52}(Zr_{2.98}Ti_{0.10}Nb_{0.07})_{3.15}[Si_{25}(O_{64.05} \cdot 8.95H_2O]_{73} \cdot 3H_2O \cdot Cl_{1.84}$

382_30. $(11.38H_2O \cdot Na_{2.98}K_{0.64})_{15}Ca_{5.33}(Fe_{1.21}Mn_{0.42})_{1.63}(Zr_{2.60}Ti_{0.17}Nb_{0.05})_{2.83}[Si_{25}(O_{63.58} \cdot 9.42H_2O]_{73} \cdot 3H_2O \cdot Cl_{1.75}$

382_28. $(12.27H_2O \cdot Na_{2.14}K_{0.58})_{15}Ca_{5.52}(Fe_{1.12}Mn_{0.42})_{1.54}(Zr_{2.90}Ti_{0.14}Nb_{0.06})_{3.10}[Si_{25}(O_{63.80} \cdot 9.20H_2O]_{73} \cdot 3H_2O \cdot Cl_{1.73}$

382_41. $(12.69H_2O \cdot Na_{1.90}K_{0.41})_{15}Ca_{5.56}(Fe_{1.11}Mn_{0.34})_{1.44}(Zr_{2.90}Ti_{0.16}Nb_{0.05})_{3.10}[Si_{25}(O_{63.52} \cdot 9.48H_2O]_{73} \cdot 3H_2O \cdot Cl_{1.74}$

382_42. $(12.04H_2O \cdot Na_{2.56}K_{0.41})_{15}Ca_{5.67}(Fe_{1.22}Mn_{0.32})_{1.54}(Zr_{2.90}Ti_{0.12}Nb_{0.06})_{3.08}[Si_{25}(O_{63.95} \cdot 9.05H_2O]_{73} \cdot 3H_2O \cdot Cl_{1.85}$

382_43. $(12.42H_2O \cdot Na_{2.36}K_{0.22})_{15}Ca_{5.62}(Fe_{1.08}Mn_{0.42})_{1.50}(Zr_{2.93}Ti_{0.08}Nb_{0.09})_{3.11}[Si_{25}(O_{63.84} \cdot 9.16H_2O]_{73} \cdot 3H_2O \cdot Cl_{1.85}$.

REE–Nb mineral occur in accessory amounts (Figs. 2, 5).

The rock has a hypidiomorphic-granular structure with euhedral albite and packetlike phlogopite crystals 0.1–1.0 mm in size. Phlogopite and albite are uniformly distributed through the rock volume, whereas calcite, as a rule, fills interstices between these minerals. Calcite inclusions are also observed in albite and phlogopite. Boundaries of major rock-forming minerals do not bear indications of corrosion.

Calcite constantly contains admixtures of Sr (~1 wt %) and Mn (0.6–0.7 wt %), as well as small, a few micrometers in size, mineral phases with predominance of strontianite. In addition, a combination of Na, La, Ce, and Sr is detected in unidentified carbonate (?) phases. Unfortunately we were unable to carry out quantitative analyses of these minerals because of their minute dimensions. In our opinion, the mode of occurrence of these mineral phases—minor dimensions, diffuse boundaries, relatively uniform distribution in calcite aggregates or localization along calcite grain boundaries and crosscutting fractures—indicate that their origin is related to recrystallization of calcite accompanied by refinement from admixtures.

Apatite occurs as barrel-shaped crystals up to 100 μm in size localized in the intergranular space, where clusters of this mineral are intergrown with calcite and zircon or occur as ingrowths into calcite and phlogopite.

Zircon is identified as euhedral dipyramidal crystals up to 100 μm in size with poorly developed prismatic faces and intergrows with albite, calcite, apatite and as inclusions in phlogopite (Fig. 5). No admixtures have been detected in zircon.

Unidentified REE–Nb mineral phases occur as isometric grains up to 10 μm in diameter. Like small calcite grains, they are related to the intergranular space between albite crystals. The chemical composition of these minerals is presented in Table 8. The high Ce and Nb contents are noteworthy.

Fe and Mn hydroxides with Si and Ba admixtures make up pseudomorphs most likely replacing pyrite and reaching a few millimeters in size. The inner part of pseudomorphs is often porous with inclusions of albite crystals and submicrometric barite segregations. Their chemical composition is variable. Local sites are composed of Fe or Fe–Mn hydroxides.

ORE MINERALIZATION

The ore mineralization occurs as large veins and cement of tectonic breccia. This is inequigranular (medium- and coarse-grained or giant-crystalline)

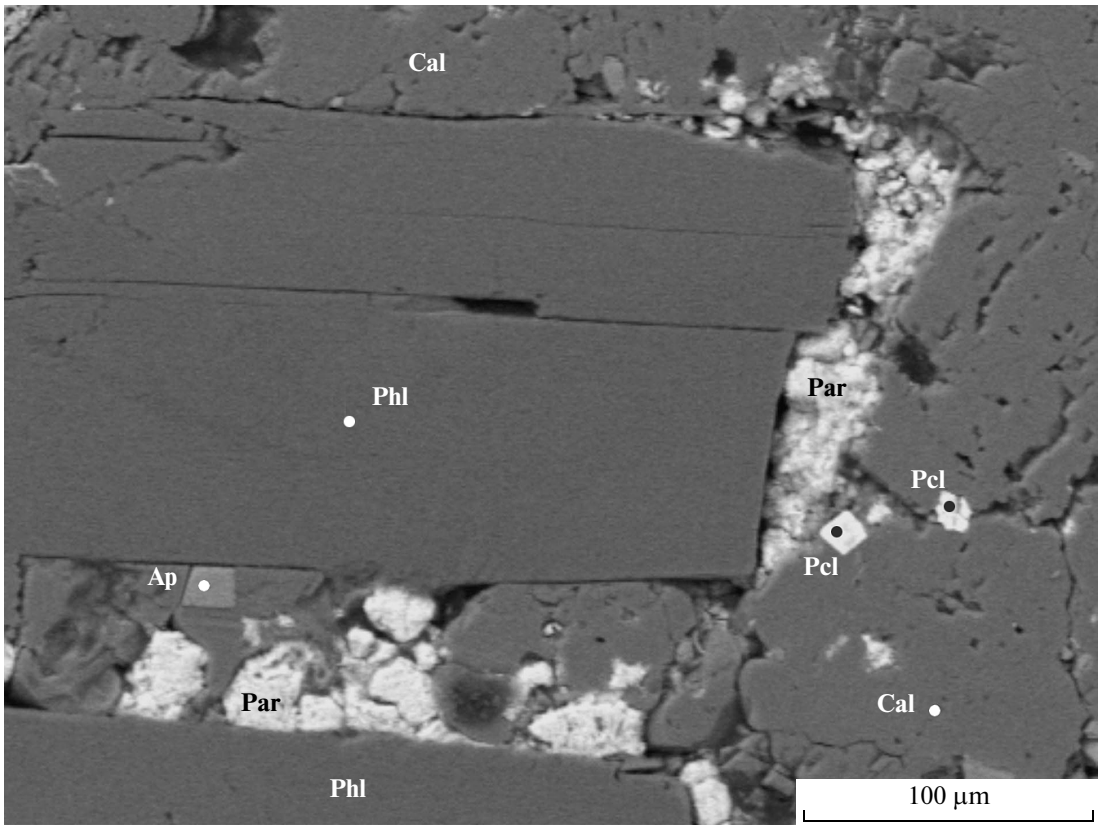


Fig. 4. REE mineralization in phlogopite–calcite carbonatite: parisite (Par) and pyrochlore (Pcl). SEM image in reflected electrons (sample 362b).

porous aggregate of fluorite and barite crystals that occupies 60–65% of the total volume. Up to 10 vol % fall on microgranular Ca-bastnaesite aggregate and up to 15–20 vol % on cavities. Fluorite, barite, and Ca-bastnaesite are major ore-forming minerals. The average chemical composition of ore is as follows (wt %): 40 CaO, ~26 F, 10–17 BaO, 5–10 SO_3, and ~7% REE.

The ore veins are characterized by a directional structure caused by the distribution of large mineral crystals along the strike of orebodies and by the elongated shape of small mineral clusters with predominance of fluorite, barite, or bastnaesite (Fig. 6). At the microlevel, the directional structure is emphasized by the orientation of phlogopite crystals (Fig. 7a). The ore is inequigranular with clear evidence of multistage crushing (Figs. 6, 7). Large crystals comprise dark purple and less frequent white with greenish or purple hue fluorite and barite in certain varieties. The crystals reach a few centimeters in size (Fig. 6); they are often euhedral and always subject to crushing (Fig. 7b).

The large crystals are incorporated into an aggregate of smaller barite and fluorite crystals or their fragments (Fig. 7). Fine-grained fluorite varies from colorless to white with a purple hue. Fluorite also occurs as inclusions in larger barite crystals. In some cases, these inclusions are located along zones of barite growth (Fig. 7c).

The lenticular and amoeba-like aggregates of Ca-bastnaesite microcrystals in association with sporadic barite, K-feldspar, and fluorite occupy a subordinate position in rock (Fig. 8). Fluorite locally cements bastnaesite. Depending on general grain size of rock, bastnaesite aggregates vary in size from a few millimeters to a few centimeters.

Phlogopite and K-feldspar are constantly present in the ore. Quartz grains are noted. Pyrochlore and Nb-bearing rutile are identified in SEM images. Rhabdophane, florencite, and chalcedony are late superposed minerals. Cementation of rock with Fe and Mn hydroxides containing Ba and Pb as admixtures is widespread at local sites.

The ore formation developed against the background of active tectonic processes. Some sites of orebodies resemble blastocataclasites. This similarity is emphasized by the simple mineral composition of ore, widespread crushing, and its directional structure. Comminution of early mineral aggregates if even took place always affected only ore mineral aggregates and occurred before appearance of numerous cavities. No indications of compression and mylonitization were observed in host rocks. The persistent phase composition of large ore veins and small veinlets cementing brecciated rocks is noteworthy. This feature of barite–fluorite–bastnaesite mineralization shows that the ore

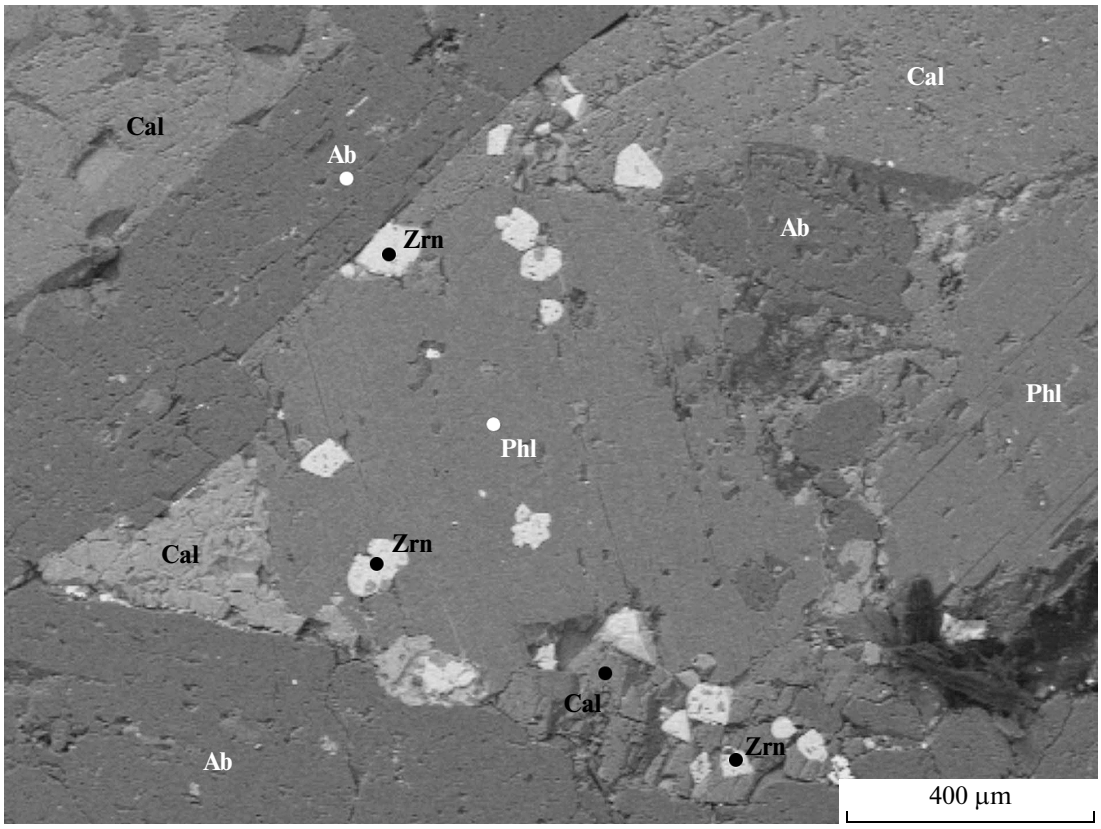


Fig. 5. Phlogopite–calcite–albite rock. SEM image in reflected electrons (sample 360). See text for explanation.

was formed by the emplacement of relatively homogeneous and mobile matter, which filled fissures and cemented zones of tectonic breccia.

The relationships of minerals in ore aggregates indicate the sequence of their formation, which at a first approximation corresponds the series: large crystals → medium- to fine-grained aggregate → bastnaesite aggregate (Fig. 2). Dark purple fluorite crystallized the first and did not contain inclusions of other minerals. Barite and pale purple fluorite crystallized later; they occupy subordinate position in respect to large crystals or their aggregates (Figs. 7, 9). In the ore

Table 8. Chemical composition of rutile and unidentified REE–Nb minerals, wt %

Component	Rutile				Unidentified minerals		
	Bastnaesite–barite–fluorite ore				Phlogopite–calcite–albite rock		
	362(7)	362(8)	374(1)	374(01)	360(6)	360(7)	360(8)
V_2O_3	0.99	0.96	–	0.94	–	–	–
Nb_2O_5	5.62	5.68	2.77	1.79	10.33	10.49	29.41
SiO_2	–	–	–	–	7.99	6.92	13.88
TiO_2	90.94	91.96	95.92	95.26	2.44	3.22	8.73
UO_2	–	–	–	–	–	1.68	4.18
Al_2O_3	–	–	–	–	–	1.23	2.25
Ce_2O_3	–	–	–	–	33.75	31.96	2.35
CaO	–	–	–	–	3.17	3.5	5.13
FeO	0.76	2.8	1.32	1.61	12	1.19	1.12
PbO	–	–	–	–	3.83	4.89	–
Total	98.31	101.4	100.01	99.6	73.51	65.08	67.05

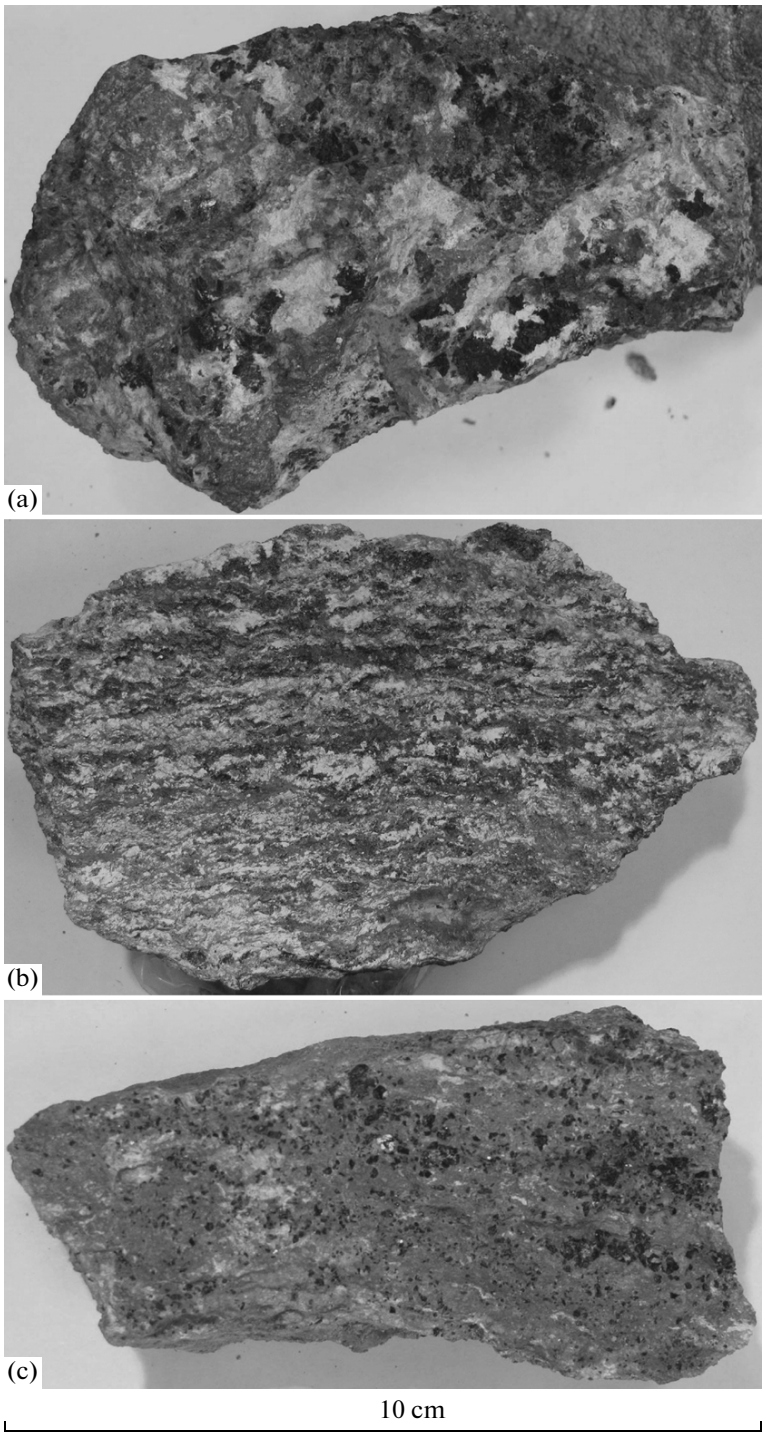


Fig. 6. Ores from Kizilcaören deposit: (a) porous giant-crystalline ore with large purple fluorite crystals and Ca-bastnaesite aggregates (sample 361); (b) porous medium-grained ore with banded structure (sample 367); (c) compact medium-grained ore with banded structure cemented by Fe hydroxides (sample 364). Dark crystals and zones are fluorite; light areas are clusters of small barite crystals and microgranular Ca-bastnaesite aggregates. Lower edge of photographs is ~10 cm.

varieties devoid of large dark purple fluorite crystals, light fluorite and barite crystallized first. Fluorite inclusions are noted in barite monocrystals.

Crushing of early crystals (Fig. 7b) is evidence for tectonic movement during ore formation. Judging by the size of crystals and subsequent fragmentation of them, K-feldspar started to crystallize simultaneously with the growth of large barite and light-colored fluorite crystals. K-feldspar crystals contain fluorite inclusions (Fig. 10) indicating that both minerals crystal-

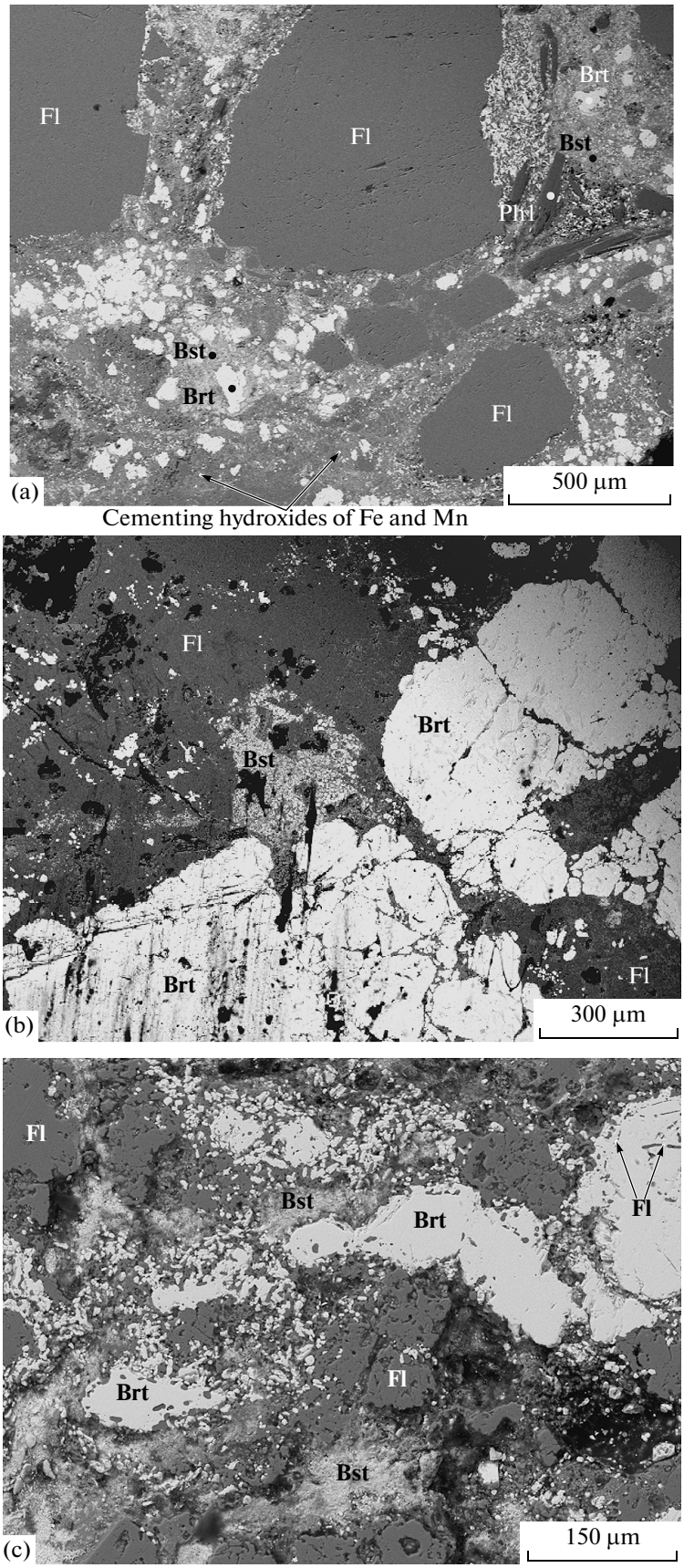


Fig. 7. Inequigranular ores from Kizilcaören deposit. SEM image in reflected electrons: (a) sample 364, (b) sample 375, and (c) sample 380a. See text for explanation.

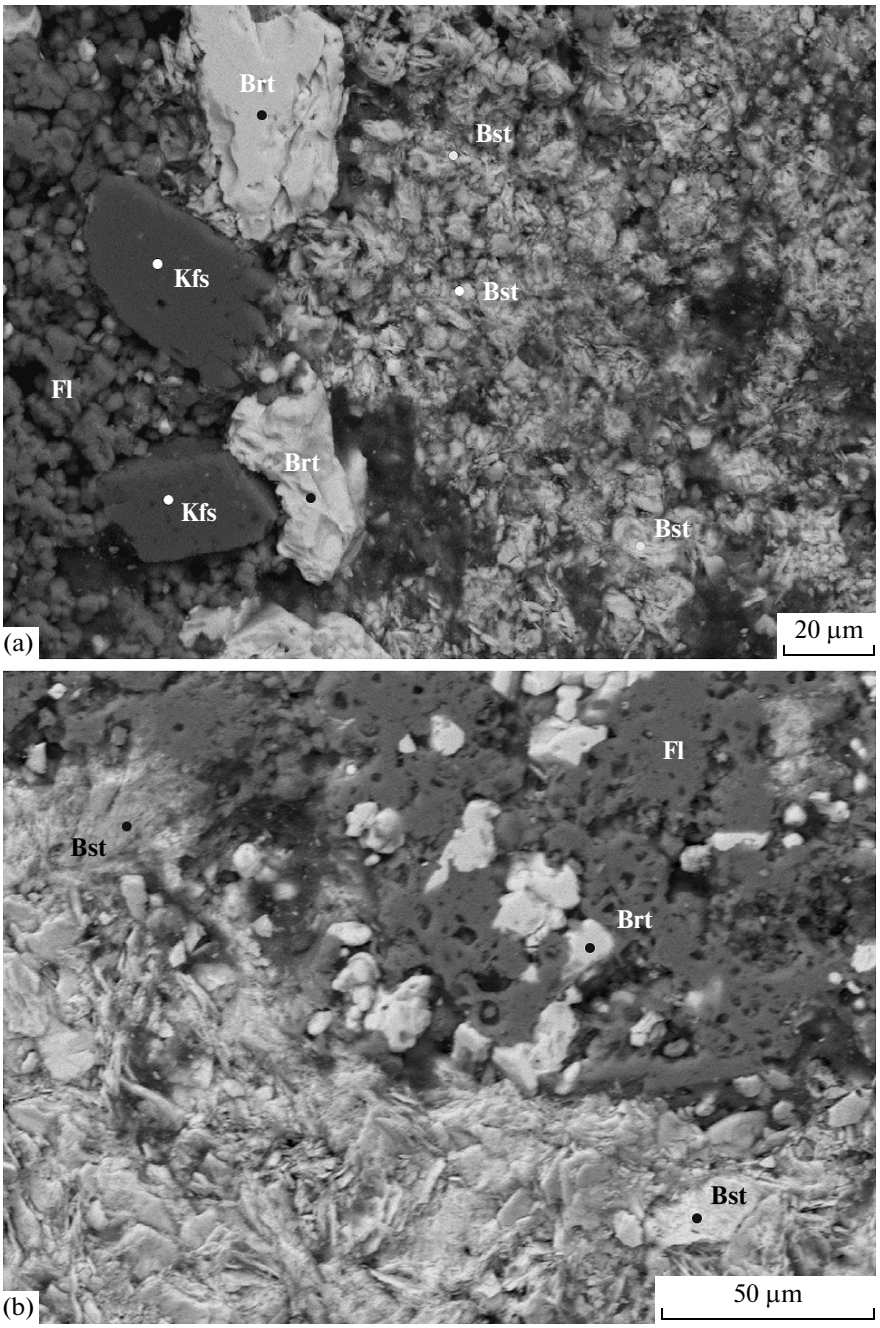


Fig. 8. Microgranular aggregates of REE minerals in ore from Kizilcaören deposit. SEM image in reflected electrons: (a) sample 362, (b) sample 379.

lized contemporaneously. Phlogopite sheets comparable with large crystals of other minerals in size are incorporated into the fine-grained barite–fluorite aggregate. Like K-feldspar, phlogopite apparently crystallized synchronously with barite and pale fluorite. Rutile occurs as inclusions in K-feldspar and thus crystallized before or simultaneously with the latter.

Ca-bastnaesite completed the endogenic mineral formation. As was mentioned above, the bastnaesite aggregate contains inclusions of barite, fluorite, and K-feldspar. The outlined sequence of fluorite, barite, and Ca-bastnaesite crystallization is exemplified in sample 367 (Fig. 9).

The formation of Fe–Mn hydroxides with Ba and Pb and rhabdophane is related to the supergene stage. Supergene svanbergite, florencite, and chalcedony have been obseved in single cases.

The mode of hydroxide occurrence includes pseudomorphs after early minerals, cement of the ore groundmass, and kidney-shaped sinters. Pyrite is the main replaced mineral (Özgenç, 1993).

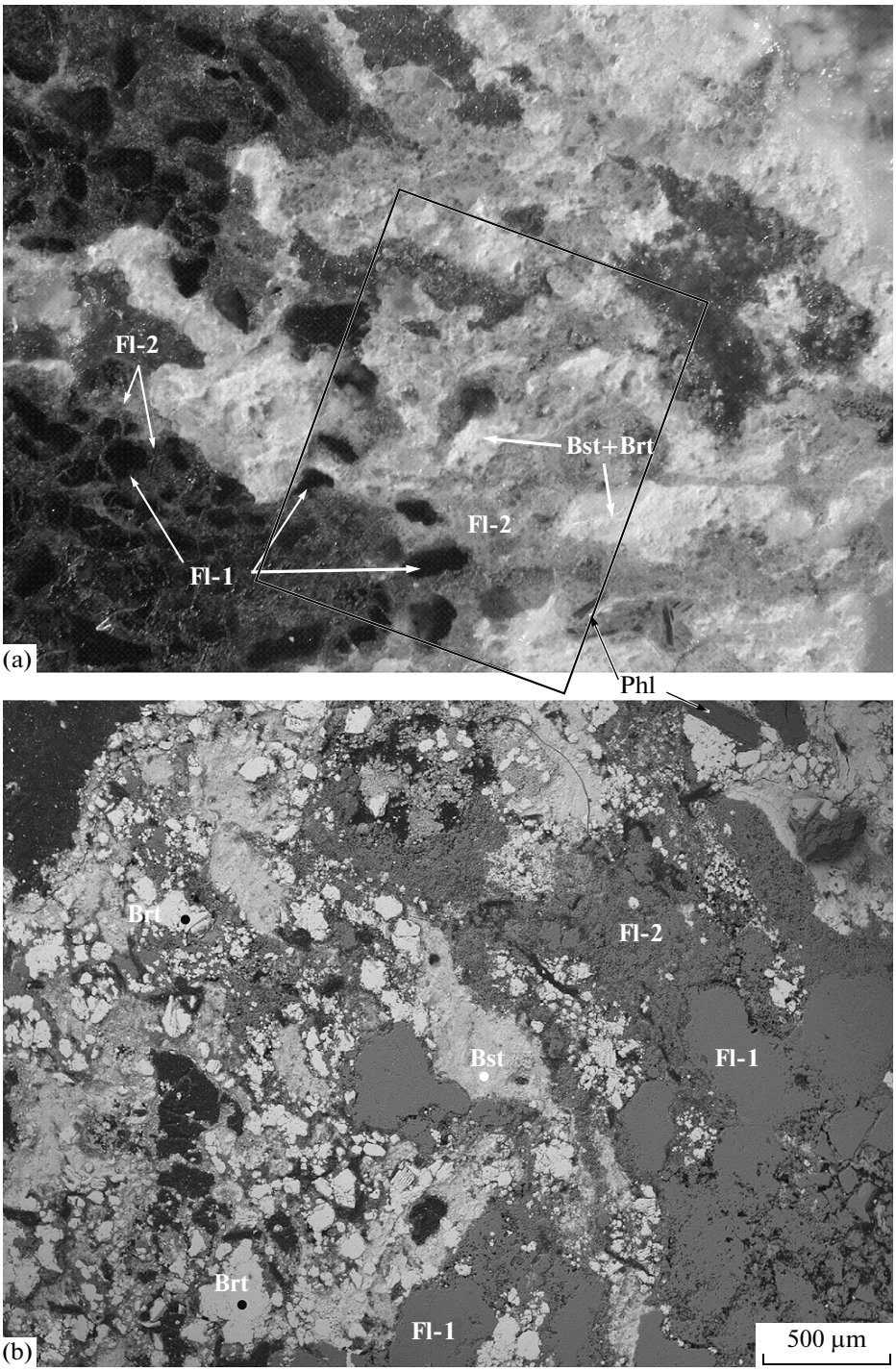


Fig. 9. Sequence of mineral formation in ore at Kizilcaören deposit, sample 367: (a) micrograph under binocular microscope and (b) SEM image in reflected electrons. Fl-1, early dark purple fluorite; Fl-2, porous aggregate of late light-colored fluorite. Rectangle in panel (a) is close-up shown in panel (b). General view of sample shown in Fig. 6b.

Cementation of the ore groundmass with Fe and Mn hydroxides is a widespread phenomenon. The ore acquired a yellowish brown color and became massive and less porous (Fig. 11). The studied samples contain 0.7–14.0 wt % $(Fe_2O_3)_{tot}$ and 0.03–0.60 MnO.

The characteristic rhabdophane spherulites are associated with cementing Fe and Mn hydroxides (Fig. 11a) and occur in cavities between small fluorite and barite crystals (Fig. 10). The rhabdophane crystals are a few micrometers in size. In addition, this mineral

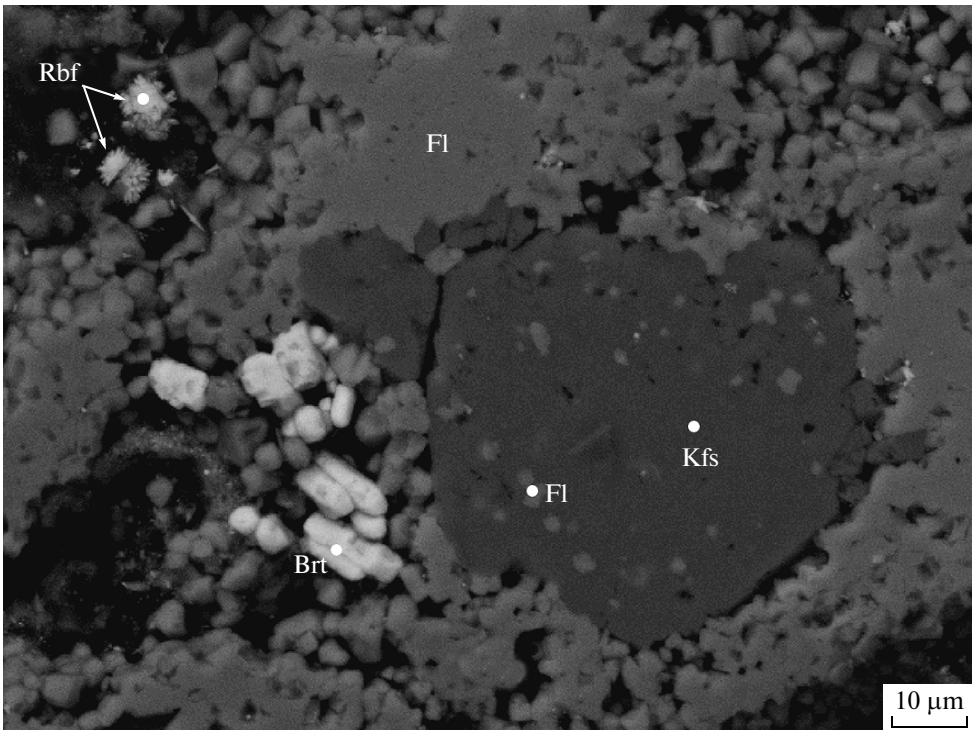


Fig. 10. Ore from Kizilcaören deposit. SEM image in reflected electrons (sample 362). Fluorite inclusions are seen in K-feldspar crystal. Numerous cavities (black) in microgranular fluorite aggregate contain rhabdophane hedgehogs.

likely coats bastnaesite crystals with the finest films, which are indiscernible in SEM images but add a variable admixture of P and occasionally Si, probably due to the occurrence of silicorhabdophane ($HCeSiPO_8 \cdot 3H_2O$).

In concluding this section, we give a description of the mineralization that cements trachyte breccia (Fig. 12), whose outcrops are known in the western part of the complex (Fig. 1, sample 374). The cementing aggregate is composed of yellowish white fine-grained fluorite occasionally with clusters of fine barite grains. Fragments of Nb-bearing rutile and zonal pyrochlore crystals are also noted (Fig. 13). An unidentified LREE carbonate locally rims rutile grains.

From 30 to 80% of the ore volume fall on fragments varying from fractions of a millimeter to a few centimeters in size (Fig. 12a). They consist of K-feldspar phenocrysts and microlites with sporadic sites where this mineral is enriched in Ba and/or Na. It should be noted that trachyte completely crystallized by the time of crushing. The superposed fluorite develops in feldspathic fragments as veinlets and amoeba-like aggregates and fills interstices between K-feldspar microlites. Fluorite is frequently accompanied by individual barite grains.

Numerous relatively uniformly distributed pores irregular in shape, as well as mineral inclusions, are observed within fragments (white spots in Fig. 12b). Barite; fluorite; in one case, monazite; thorianite; and complex Ba–Sr sulfate with predominant strontium have been identified among mineral inclusions. In addition, complex Na–Sr–Ca carbonates occasionally with LREE and Th are also observed as inclusions a few micrometers in size. They contain (wt %) 9–12 Na_2O, 10–28 SrO, up to 9 CaO, up to 14 $La_2O_3 + Ce_2O_3 + Nd_2O_3$, up to 8 F, and up to 4 ThO_2. The pores in feldspathic fragments are apparently a result of dissolution of inclusions initially occupied by a mineral-forming medium or captured mineral inclusions, e.g., complex Na–Sr–Ca–LREE carbonates.

CHEMICAL COMPOSITION OF ROCK-FORMING AND ACCESSORY MINERALS

The chemical compositions of rock-forming and accessory minerals from the studied rock complex are considered in this section.

Feldspars in rocks except for phonolite (see subsection "Alkaline silicate rocks") are represented by a pure potassium variety or albite. K-feldspar from trachyte and fluorite–barite–bastnaesite ore locally contains up to 1 wt % Na_2O and 3 wt % BaO; however, in most cases, the contents of these elements are below the detection limits of the analytical techniques. No admixtures have been detected in albite from the phlogopite–calcite–albite rocks.

Barite from orebodies also does not contain detectable admixtures. Barite from calcite-bearing rocks contains up to 1 wt % Sr.

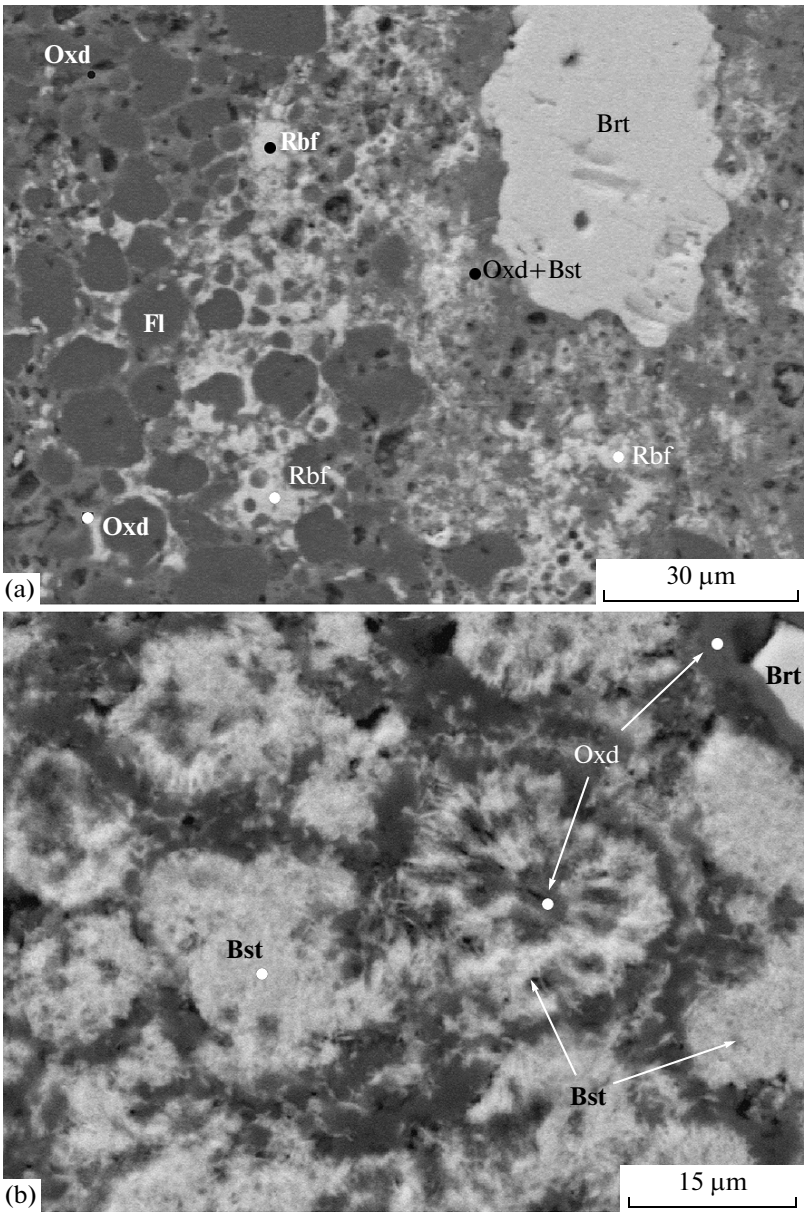


Fig. 11. Supergene Fe and Mn hydroxides (Oxd) and rhabdophane (Rbd) in ore from Kizilcaören deposit. SEM image in reflected electrons: (a) sample 370 and (b) sample 375).

LREE fluorocarbonates are widespread in the ore and were detected in phlogopite–calcite rock and phonolite.

The LREE fluorocarbonates from ore contain up to 10 wt % Th and 5.6 wt % Sr (Table 9). The 2REE → Th + (Ca,Sr) scheme of isomorphism has apparently been realized. The recalculation of chemical compositions of the minerals shows that they are intermediate between compositions of bastnaesite and parisite.

The LREE fluorocarbonate from phlogopite–calcite rock is represented by parisite. Thorium has not been detected, and Sr admixture (1.6–1.8 wt %) has been constantly noted. Submicrometric LREE fluorocarbonate grains (probably, parisite) occur in the groundmass of phonolite.

Rhabdophane occurs in ore and phlogopite–calcite–albite rock as a supergene mineral. The chemical elements of the host matrix are commonly recorded in analyses of this mineral (Table 10); however, analysis 370(5) of a relatively large (~5 μm) crystal is satisfactorily recalculated to the rhabdophane formula $(Ca_{0.09}Sr_{0.07}Th_{0.06})_{0.22}(Ce_{0.4}La_{0.18}Nd_{0.16}Pr_{0.03})_{0.77}(PO_4)_{1.02}\cdot 0.96H_2O$. Thorium is constantly detected in this mineral, and its concentration reaches 7 wt %. Like Ca-bastnaesite, rhabdophane is characterized by a 2REE → Th + (Ca,Sr) scheme of isomorphism. In certain

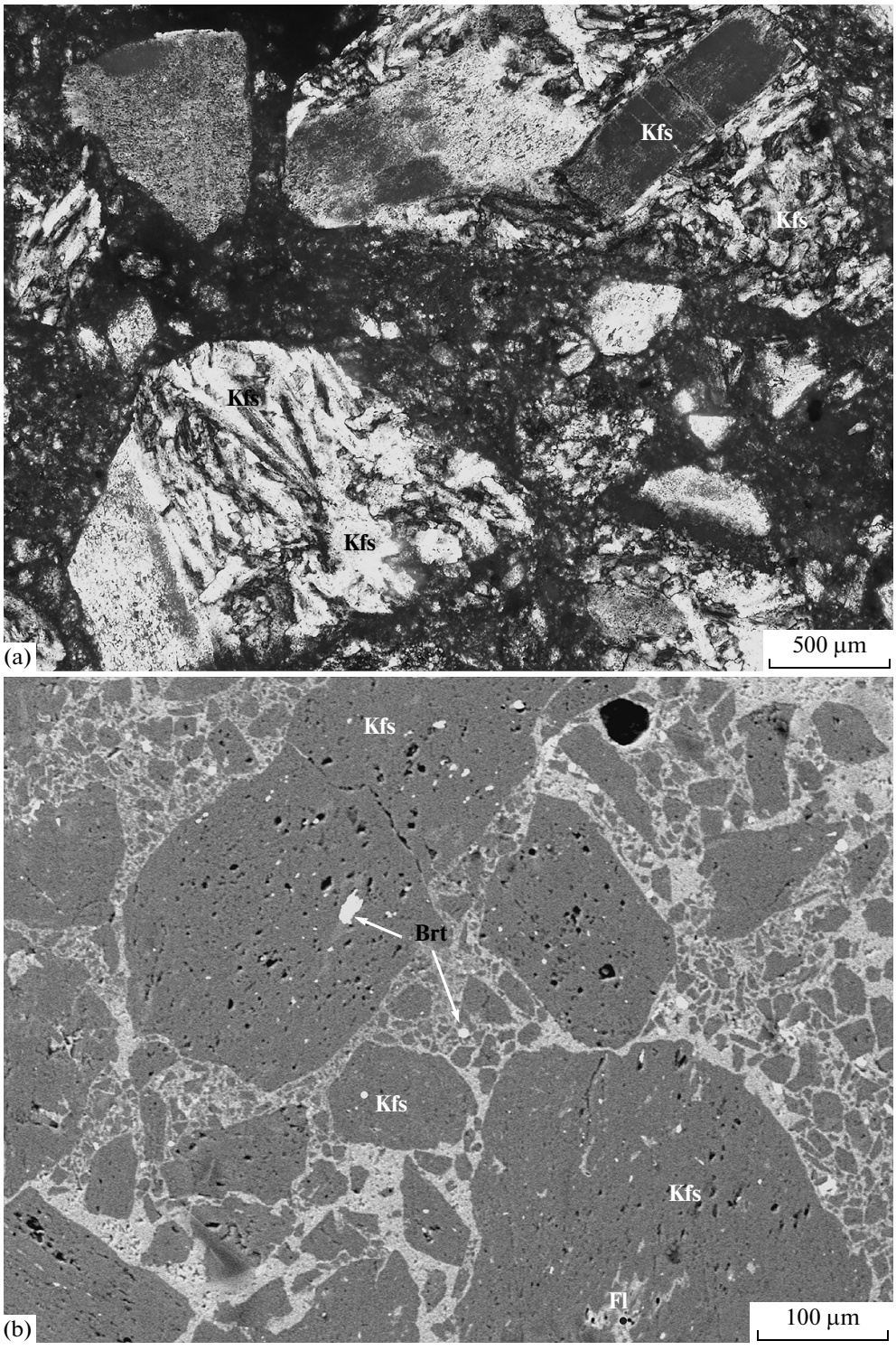


Fig. 12. Trachyte breccia with barite–fluorite cement (sample 374): (a) photomicrograph in transmitted light, crossed polars; phenocrysts and microlites of groundmass are seen in fragments; (b) SEM image in reflected electron; numerous pores and mineral inclusions are seen in fragments.

cases, U (up to 1 wt %), Si, or Ca are noted. In these cases, we are apparently dealing with silicorhabdophane $HCe_2SiPO_8 \cdot 3H_2O$ or Ca-rhabdophane $CaCe[HPO_4][PO_4] \cdot 2H_2O$.

Apatite is relatively abundant in calcite-bearing rocks and has been identified as a mineral inclusion in pyroxene from phonolite. This is fluorapatite containing up to 3.6 wt % Sr (Table 10).

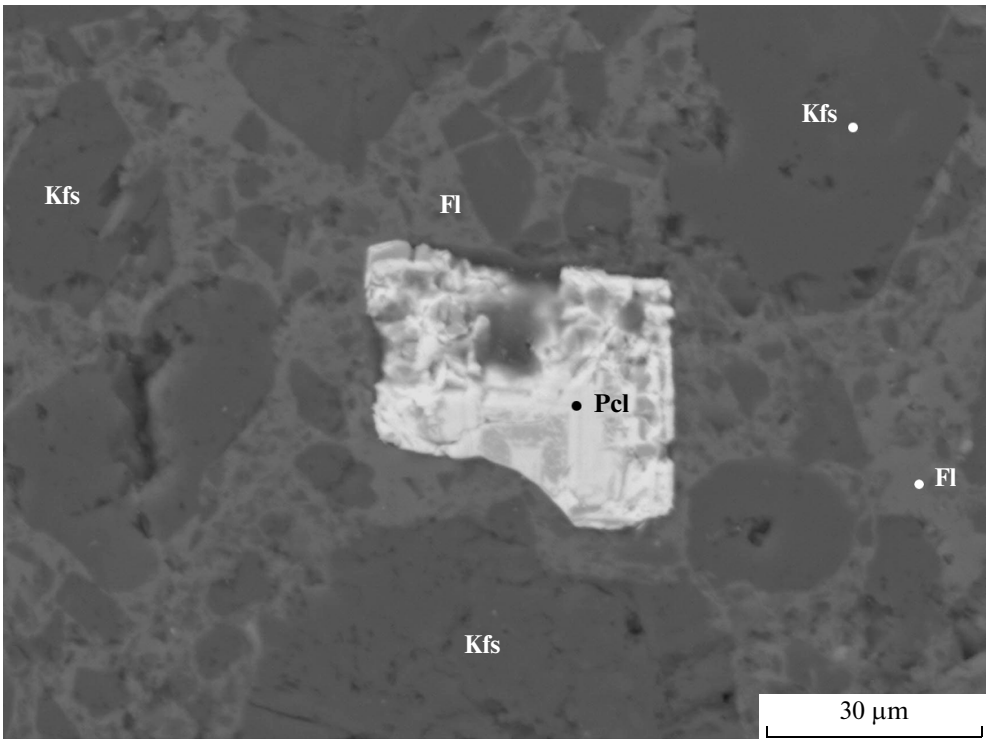


Fig. 13. Fragment of zonal pyrochlore crystal incorporated into barite–fluorite cement of trachyte breccia.

Svanbergite $SrAl_3[PO_4][SO_4](OH)_6$ has been identified from its chemical composition (Table 10). This mineral is intergrown with Fe hydroxide and rhabdophane as submicrometric segregation with diffuse boundaries.

Fe–Mg micas occur in all rocks. In chemical composition (Table 11), they are related to the annite–phlogopite or siderophyllite–eastonite series. Phlogopite and eastonite end members are absolutely predominant. As a rule, only a single mica variety is contained in the rock; however, both varieties—large phlogopite and small eastonite crystals—have been detected in the phlogopite–calcite rock.

Pyrochlore occurs in phlogopite–calcite carbonatite, in cement of trachyte breccia, and in one ore sample as intergrowths with Nb-rutile, fluorite, barite, and Ca-bastnaesite. Pyrochlore crystals are a few tens of micrometers in size. Their morphology is shown in Figs. 4 and 13.

The most reliable chemical compositions of pyrochlore are given in Table 12. The formulas have been calculated using the Borodin method (Borodin and Nazarenko, 1957) on the basis of (Nb + Ta + Ti) = 2. Pyrochlore, as a rule, reveals a deficiency in cations and high Pb concentration. In the latter case, we are dealing with hydroxylplumbopyrochlore. Pyrochlore from phlogopite–calcite carbonatite contains Na and varies in Pb and Ca contents. Its chemical composition corresponds to hydroxylcalciopyrochlore. These chemical variations show that almost all analyzed pyrochlores have been subjected to late (supergene?) alteration.

Rutile was found in ore sample 362 as an intergrowth with pyrochlore and in barite–fluorite cement of trachyte breccia. The rutile crystals are a few tens of micrometers in size; Fe, V, and Nb admixtures were established in this mineral (Table 8).

The local analysis results for *Mn and Fe hydroxides* are shown in Table 13. Fe hydroxide (hydrogoethite?) with Si, Al, Ca, and Mn admixtures are contained in groundmass of ore and as sinter aggregates. Mn hydroxides (psilomelane?) with Fe and Ba admixtures are identified in veinlets and zone of cementation nearby. Pb–Mn hydroxide (coronadite?) was established in one case. Pseudomorphs are composed of Fe and Mn hydroxides.

DISCUSSION

The results of the performed study of earlier published data allow us to answer certain questions on the origin and formation conditions of the Kizilcaören fluorite–barite–REE deposit.

Genesis of Studied Rocks and Their Interrelations

Subvolcanic phonolite related to the Kizilcaören Complex is typical alkaline silicate rock of the K–Na series with foid contents exceeding 30 vol %; the Na_2O and K_2O contents are 7.5 and 5.44 wt %, respectively.

Table 9. Chemical composition of REE fluorocarbonates, wt %

Component	Phlogopite–calcite carbonatite				Bastnaesite–barite–fluorite ore			
	362-b(11)	362-b(12)	362-b(15)	362-b(17)	379(19)	379(21)	379(18)	367(1)
$CO_{2\,calc}$	19.98	20.55	19.25	21.0	19.0	18.6	17.7	17.9
ThO_2	–	–	–	–	–	2.33	10.14	0.68
UO_2	–	–	–	–	–	–	–	–
La_2O_3	18.31	19.55	18.04	19.67	16.49	21.92	16.03	26.53
Ce_2O_3	22.31	22.45	22.74	23.4	23.32	25.19	19.07	26.51
Pr_2O_3					2.58	1.5	0	1.43
Nd_2O_3	5.58	4.09	5.88	5.14	4.54	5.26	5.61	3.43
CaO	8.77	9.4	7.65	9.33	4.98	2.9	4.85	2.3
SrO	1.62	1.81	1.69	1.7	5.89	3.42	2.83	0.91
F	5.75	5.91	5.54	6.04	5.45	6.73	6.15	6.8
Total	82.32	83.76	80.79	86.28	82.3	87.85	82.38	86.49
F + Cl + S = O	2.42	2.48	2.33	2.54	2.29	2.83	2.58	2.86
Total 2	79.91	81.28	78.46	83.74	79.96	85.02	79.8	83.63
Formula coefficient								
CO_2	*3.00*	*3.00*	*3.00*	*3.00*	*1*	*1*	*1.01*	*1*
La^{3+}	*0.74*	*0.77*	*0.76*	*0.76*	*0.23*	*0.32*	*0.25*	*0.40*
Ce^{3+}	*0.90*	*0.88*	*0.95*	*0.90*	*0.33*	*0.36*	*0.29*	*0.40*
Pr^{3+}					*0.04*	*0.02*	*0*	*0.02*
Nd^{3+}	*0.22*	*0.16*	*0.24*	*0.19*	*0.06*	*0.07*	*0.08*	*0.05*
REE total	*1.86*	*1.81*	*1.95*	*1.85*	*0.66*	*0.77*	*0.62*	*0.87*
Ca^{2+}	*1.03*	*1.08*	*0.94*	*1.05*	*0.21*	*0.12*	*0.22*	*0.10*
Sr^{2+}	*0.10*	*0.11*	*0.11*	*0.10*	*0.13*	*0.08*	*0.07*	*0.02*
Th^{4+}						*0.02*	*0.1*	*0.01*
U^{4+}								
F^{1-}	*2.00*	*2.00*	*2.00*	*2.00*	*0.66*	*0.84*	*0.81*	*0.88*

Component	Bastnaesite–barite–fluorite ore								
	367(2)	378(1)	375(3)	375(2)	362(12)	362(3)	362(2)	361(13)	361(1)
$CO_{2\,calc}$	12.8	18.9	21.0	18.5	17.55	15.9	15.9	18.3	14.0
ThO_2	–	–	7.11	6.01	1.3	3.2	3.55	4.13	–
UO_2	–	–	–	–	–	0.4	0.22	–	–
La_2O_3	17.51	24.71	12.04	11.35	11.55	20.64	22.08	10.18	14.99
Ce_2O_3	18.32	30.88	27.43	25.35	40.47	20.16	24.48	40.78	21.77
Pr_2O_3	1.47	2.13	3.29	2.14	0.53	1.35	2.65		
Nd_2O_3	2.87	5.51	14.28	11.93	3.06	4.69	6.3	2.53	4.18
CaO	1.99	2.39	5.76	4.92	2.87	2.3	2.97	4.01	3.79
SrO	1.03	–	–	–	0.28	2	2.28	–	–
F	4.65	7.3	7.72	6.72	6.6	5.89	6.9	6.8	4.74
Total	60.64	94.42	98.63	86.92	86	76.53	87.33	86.73	63.47
F + Cl + S = O	1.95	4.12	3.24	2.82	2.77	2.47	2.9	2.86	1.99
Total 2	58.69	90.3	95.39	84.1	83.23	74.06	84.43	83.87	61.48

Table 9. (Contd.)

Component	Bastnaesite–barite–fluorite ore								
	367(2)	378(1)	375(3)	375(2)	362(12)	362(3)	362(2)	361(13)	361(1)
Formula coefficient									
CO_2	*1*	*1*	*1*	*1*	*1.00*	*1.01*	*1*	*1.01*	*1*
La^{3+}	*0.37*	*0.35*	*0.16*	*0.17*	*0.18*	*0.35*	*0.32*	*0.15*	*0.29*
Ce^{3+}	*0.38*	*0.44*	*0.35*	*0.37*	*0.62*	*0.34*	*0.35*	*0.6*	*0.42*
Pr^{3+}	*0.03*	*0.03*	*0.04*	*0.03*	*0.01*	*0.02*	*0.04*		
Nd^{3+}	*0.06*	*0.08*	*0.18*	*0.17*	*0.05*	*0.08*	*0.09*	*0.04*	*0.08*
REE total	*0.84*	*0.9*	*0.73*	*0.74*	*0.85*	*0.79*	*0.8*	*0.79*	*0.79*
Ca^{2+}	*0.12*	*0.1*	*0.22*	*0.21*	*0.13*	*0.11*	*0.12*	*0.17*	*0.21*
Sr^{2+}	*0.03*				*0.01*	*0.05*	*0.05*		
Th^{4+}			*0.06*	*0.05*	*0.01*	*0.03*	*0.03*	*0.04*	
U^{4+}						*0.00*	*0.00*		
F^{1-}	*0.84*	*0.89*	*0.85*	*0.85*	*0.87*	*0.87*	*0.85*	*0.87*	*0.79*

Content of CO_2 is calculated.

Table 10. Chemical composition of phosphates, wt %

Component	Rhabdophane from bastnaesite–barite–fluorite ore							Svanbergite from ore	Apatite from calcite-bearing ore			
	362(4)	362(5)	364(8)	364(9)	370(5)	370(14)	370(15)	374(2)	364(7)	360(8)	362-b(7)	362-b(10)
SiO_2	–	–	–	–	–	1.58	–	1.17	–	–	–	–
Al_2O_3	–	–	1.86	1.92	–	1.49	1.49	–	26.01	–	–	–
P_2O_5	32.27	27.91	30.77	20.71	30.42	20.41	30.22	29.4	21.91	42.52	44.14	40.34
CaO	~~10.95~~	~~15~~	2.33	2.04	2.1	1.67	2.03	2.64	3.52	51.75	52.6	50.06
SrO	1.57	1.25		1.85	3.2		2.2	0	13.21	1.9	3.43	3.58
BaO	–	–	~~4.6~~	–	–	–	–	–	2.82	–	–	–
FeO	–	–	–	–	0.85	~~21.8~~	~~8.35~~	–	1.19	–	–	–
La_2O_3	14.21	15.2	19.82	20.95	12.15	7.01	9.01	15.63	–	–	–	–
Ce_2O_3	18.26	19.83	23.83	24.78	27.61	16.54	20.73	13.9	–	–	–	–
Pr_2O_3	1.61	1.55	2.21	2.05	2.4	2.28	1.76	2.71	–	–	–	–
Nd_2O_3	5.82	4.92	5.11	4.43	11.42	7.67	9.82	11.46	–	–	–	–
ThO_2	5.81	3.35	–	–	7.05	4.98	6.7	2.73	–	–	–	–
UO_2	0.48	0.7	–	1.19	–	–	0.77	–	–	–	–	–
F	~~4.95~~	~~8.22~~	1.57	2.97	–	–	–	–	–	5.24	5.33	3.79
SO_3		0.83	~~3.14~~	0.86	–	0.82	–	–	3.65	–	–	–
Total	95.93	98.76	95.24	83.75						101.41	105.5	97.77
O = F	2.08	3.45	0.66	1.25						2.2	2.24	1.59
Total 2	93.85	95.31	94.58	82.5	97.2	86.25	93.08	79.64	72.31	99.21	103.26	96.18

362(4) and 362(5), intergrowths of acicular crystals (hedgehogs) in cavities of fluorite matrix; 364(8) and 364(9), intergrowths with Fe and Mn hydroxides, svanbergite, and probably Ca-bastnaesite; 370(5), 370(14), and 370(15), intergrowths with Fe and Mn hydroxides and 370(15), additionally with LREE fluorocarbonate; 374(2) segregation in veinlet between K-feldspar, barite, and fluorite grains. Concentrations of chemical elements entrapped from host matrix are marked by strikeout.

Table 11. Chemical composition of Fe–Mg mica, wt %

Component	Bastnaesite–barite–fluorite ore					Phlogopite–calcite carbonatite				Phlogopite–calcite–albite rock		
	375(1)	364(6)	370(1)	362(6)	380a(31)	362-b(13)	362-b(21)	362-b(23)	362-b(11)	360(25)	360(212)	360(94)
SiO_2	47.00	40.35	46.40	41.36	43.46	49.69	48.61	43.59	42.73	38.12	40.29	40.95
TiO_2	–	–	0.94	0.62	1.03	–	–	–	–	0.79	1.02	0.81
Al_2O_3	4.68	8.65	6.80	7.54	6.88	2.83	2.99	6.04	4.20	9.48	8.95	9.33
FeO	2.48	4.37	4.70	5.00	7.56	2.69	2.74	4.54	4.76	5.42	4.80	5.28
MnO	–	0.49		0.66	1.31	–	–	–	–	0.58	0.58	
MgO	21.25	21.35	21.52	19.06	17.82	21.81	22.55	21.67	20.53	20.01	20.32	22.75
Na_2O	–	–	–	–	–	–	–	–	–	0.61	–	–
K_2O	11.27	10.53	11.81	11.11	11.44	11.69	11.69	11.41	10.33	10.08	10.92	10.42
F	6.57	5.85	6.13	6.49	7.05	6.99	7.05	3.99	6.30	4.88	5.66	6.66
Total	93.25	91.59	98.30	91.84	96.55	95.70	95.63	91.24	88.85	89.97	92.54	96.20
XSdph	*4.92*	*1.38*	*3.63*	*3.99*	*6.03*	*6.47*	*2.43*	*0.12*	*0*	*0*	*1.69*	*0*
XEast	*75.14*	*10.84*	*29.61*	*23.96*	*21.56*	*93.53*	*35.72*	*1.05*	*0*	*0*	*11.35*	*0*
XAnn	*1.22*	*9.94*	*7.28*	*10.29*	*15.82*	*0*	*3.94*	*10.39*	*11.50*	*14.40*	*11.25*	*11.51*
XPhl	*18.72*	*77.83*	*59.48*	*61.75*	*56.59*	*0*	*57.90*	*88.44*	*88.50*	*85.60*	*75.71*	*88.49*

Table 12. Chemical composition of pyrochlore, wt %

Component	Bastnaesite–barite–fluorite ore			Trachyte breccia	Phlogopite–calcite carbonatite		
	362(9)	362(10)	362(11)	374(2)	362-b(16)	362-b(8)	362-b(9)
Nb_2O_5	36.29	38.52	34.2	52.02	43.95	50.75	54.39
SiO_2	–	–	–	–	2.51	2.94	1.28
TiO_2	6.17	6.09	6.65	5.04	7.57	7.93	8.92
ThO_2	–	–	–	2.27	–	–	–
UO_2	–	–	–	1.71	1.57	1.91	1.67
Ce_2O_3	2.67		6.43	3.31	2.7	5.05	–
Nd_2O_3	–	–	–	0.51	–	–	–
CaO			3.57	5.41	9.4	17.53	16.65
SrO	–	–	–	–	1.35	2.99	1.09
PbO	40.77	39.62	37.81	20.08	15.85	4.92	–
Na_2O	–	–	–	–	1.19	1.76	7.55
Total	85.9	84.23	88.66	90.35	86.09	95.78	91.55

SiO_2 was not taken into account in calculations.
362(9). $(Pb_{1.04}Ce_{0.09})_{1.14}(Nb_{1.56}Ti_{0.44})_2(O_{4.92}OH_{2.08})_7$
362(10). $Pb_{0.97}(Nb_{1.58}Ti_{0.42})_2(O_{4.52}OH_{2.48})_7$
362(11). $(Pb_{0.99}Ca_{0.37}Ce_{0.23})_{1.60}(Nb_{1.51}Ti_{0.49})_2(O_{5.94}OH_{1.06})_7$
374(2). $(Ca_{0.42}Pb_{0.40}Ce_{0.09}Th_{0.04}U_{0.03}Nd_{0.01})_{0.99}(Nb_{1.72}Ti_{0.28})_2(O_{4.93}OH_{2.07})_7$
362-b(16). $(Ca_{0.79}Pb_{0.33}Na_{0.18}Ce_{0.08}Sr_{0.06}U_{0.03})_{1.41}(Nb_{1.55}Ti_{0.45})_2(O_{5.44}OH_{1.56})_7$
362-b(8). $(Ca_{1.03}Na_{0.24}Pb_{0.09}Ce_{0.13}Sr_{0.12}U_{0.03})_{1.78}(Nb_{1.59}Ti_{0.41})_2(O_{6.35}OH_{0.65})_7$
362-b(9). $(Ca_{1.14}Na_{0.94}Sr_{0.04}U_{0.02})_{2.10}(Nb_{1.57}Ti_{0.43})_2(O_{5.96}OH_{1.04})_7$

Table 13. Chemical composition of Fe and Mn hydroxides, wt %

Component	Bastnaesite–barite–fluorite ore								Calcite-bearing rock			
	375(4)	375(5)	360(2)	361(10)	361(11)	379(20)	366(22)	379(17)	362-b(3)	362-b(14)	362-b(6)	360(4)
	GM	GM	PM	SN	SN	CV	GM	CV	PM	PM	CV	PM
SiO_2	5.79	6.81	10.51	4.28	4.51	–	–	–	3.2	3.66	–	5.4
Al_2O_3	3.5	2.59	1.33	–	–	–	–	–	–	–	–	–
CaO	0.54	0.5	0.92	–	0.39	0.86	1.0	–	–	–	0.93	2.72
Fe_2O_3	78.92	64.14	68.38	76.06	66.41	2.78	0	0	77.38	76.13	1.58	27.92
MnO	–	–	–	3.43	2.27	51.42	62.78	41.26	3.16	2.37	51.73	23.86
BaO	–	–	–	–	–	10.78	11.43	2.55	–	–	10.19	3.86
SrO	–	–	–	–	–	–	–	–	–	–	0.97	–
PbO	–	–	–	–	–	–	–	18.52	–	–	1.69	–
ZnO	–	–	–	0.81	2.42	–	–	–	1.82	1.43	1.16	–
MoO_3	–	–	–	–	1.7	–	–	–	–	–	–	–
SO_3	–	–	–	–	0.25	0.93	–	–	–	–	–	–
V_2O_3	–	–	–	–	0.78	–	–	–	–	–	–	–
K_2O	–	–	–	–	–	–	0.93	–	–	–	–	–
Ce_2O_3	–	–	–	–	–	–	–	–	–	–	–	4.88
MgO	–	–	–	–	–	–	–	–	–	–	–	2.2
Total	88.75	74.04	81.14	84.58	78.73	66.77	76.14	62.33	85.56	83.59	68.25	70.84

Mode of hydroxide occurrences: GM, cement of groundmass; CV, cementing veinlet; SN, kidney-shaped sinter; PM, pseudomorph.

The compositional evolution of minerals in phonolite is characterized by an increase in alkalinity (enrichment in aegerine end member in pyroxene) and enrichment in volatile components (H_2O, Cl, S) at the late stage of melt crystallization. An extremely hydrous mineral of the eudialyte group is contained in phonolite, indicating that the residual melt was enriched in H_2O and Cl. Pyrite and galena microinclusions in groundmass are evidence for enrichment of residual melt in sulfur. Early nepheline was replaced by analcime and minerals of sodalite and zeolites groups containing H_2O.

Substantially carbonate phlogopite–calcite rocks contain phlogopite, apatite, pyrochlore, and parisite inherent to carbonatites. The chemical composition of these minerals is also typical of carbonatites: elevated Sr contents in calcite and apatite; the later is also enriched in fluorine. The homogeneous structure of rocks throughout outcrops corroborates their magmatic origin and allows us to classify these rocks as carbonatites. The same criteria make it possible to believe that the phlogopite–calcite–albite rock is genetically related to phlogopite–calcite carbonatite. However, the origin of pure albite contained in these rocks remains ambiguous.

The major primary minerals in the ore at this deposit are barite, fluorite, and bastnaesite. The suggestion on leaching of readily soluble mineral phases from the rocks, which acquired a porous structure, so far remains questionable. Phlogopite, K-feldspar, and rutile crystals are constant admixtures in ore. The same minerals with similar chemical composition have been identified in phlogopite–calcite–albite rock and carbonatite.

The supergene mineralization widespread in ore at the Kizilcaören deposit is primarily represented by Fe and Mn hydroxides containing Ba and Pb and by rhabdophane as an REE phosphate. The large number of supergene minerals poses the question on the source of chemical elements concentrated therein. The close spatial association of superposed mineralization with orebodies assumes that the ore itself was a source of elements that are mobile under supergene conditions; however, except for Ba and LREE, these elements are absent in the ore. Taking into account the porous structure of ore, it cannot be ruled out that the primary ore contained carbonates of the $MnCO_3$–$CaCO_3$ and $MnCO_3$–$FeCO_3$ series, as well as a double salt of the $Ca(Mg–Fe)(CO_3)_2$ type. Galena, which was identified in phonolite, could have been a source of lead. Phosphorus could have been taken from apatite and monazite.

In general, the through minerals that crystallized in two or more types of rocks and contained in the ore are known (Fig. 2). For example, phlogopite is contained in carbonatite, phlogopite–calcite–albite rock, and bastnaesite–barite–fluorite ore. Pyrochlore is noted in carbonatite, ore, and barite–fluorite cement of trachyte breccia. Alkali feldspar (K and Na), barite, REE

fluorocarbonates (parisite, Ca-bastnaesite), and apatite are through minerals as well. The elevated Nb and Ce concentrations in the phlogopite–calcite–albite rock are related to other minerals, which so far remains unidentified (Table 8).

As concerns interrelations of ore with carbonate, carbonate–silicate, and silicate (phonolite) rocks, it should be noted that all of them are localized in a small (~30 km^2) territory and in the same permeable tectonic suture. According to the geochronological data, carbonatite, phlogopite–calcite–albite rock, and phonolite formed almost synchronously 24–25 Ma ago. The through minerals—phlogopite, pyrochlore, LREE fluorocarbonates, etc.—occur in various rocks of the complex. The phlogopite–calcite–albite rock is a connecting link between phonolite, on the one hand, and carbonatite and bastnaesite–barite–fluorite ore, on the other. All this is evidence for genetic relations between the considered rocks.

Mineral Formation Conditions

The aggregate state of ore-forming matter and temperature of ore formation are of great importance for understanding the origin of bastnaesite–barite–fluorite ore. The texture and structure of ore and morphology of orebodies show that their formation was a result of injection of an ore-forming medium enriched in early fluorite crystals and locally barite into crush zones. Variously oriented fragments of host rocks are observed in the contact zones of orebodies. The ore crystallized from the continuously moving medium, and this process was accompanied by fragmentation of early dark purple fluorite crystals and smaller crystals of light-colored fluorite and barite. Microgranular aggregates of Ca-bastnaesite, which occupy a subordinate position in respect to large fluorite and barite crystals, formed at the final stage of ore formation.

The fluid inclusions in carbonatite and ore from the Kizilcaören deposit were studied by Delaloye and Özgenç (1983), Gültekin et al. (2003), and Altuncu (2009). The homogenization temperature of fluid (?) inclusions in calcite from carbonatite is estimated at 550°C (Delaloye and Özgenç, 1983). The ore minerals started to crystallize from supercritical fluid at 436°C and continued to grow down to 113°C (the homogenization temperature of fluid inclusions is given from here on). The highest-temperature inclusions in quartz and early fluorite are distinguished by the highest salinity (up to 22.4 wt % NaCl equiv) and homogenize into gas. Starting at 330°C, most inclusions are homogenized into liquid and the salinity of the fluid varies from 15 to 1 wt % NaCl equiv. The main temperature range of mineral formation is 300–200°C. Ca-bastnaesite crystallized at 300–150°C; the homogenization temperature of fluid inclusions in barite is 206–140°C. The lowest homogenization temperature of primary and secondary fluid inclusions was noted at 105°C. Salinity of low-temperature solutions rarely exceeds 5 wt % NaCl equiv.

Gültekin et al. (2003) proposed the following genetic model of the deposit. Silicate trachytic and phonolithic melts formed along with carbonatite liquid, and a fluid enriched in SO_2 and HF was separated from this liquid. Silicification and crystallization of plagioclase proceeded at this stage in zones of brecciation. The fluorite–barite–REE ore was formed from the fluid, which boiled up and was characterized by high salinity. When ascending to a higher level, the high-salinity fluid mixed with low-salinity meteoric water. The main body of ore matter crystallized from this mixed fluid. Thus, the authors of the cited publication refer the Kizilcaören deposit to the veined epithermal type of mineralization.

Geochronological and mineralogical evidence for interrelations between phonolite, feldspar–carbonate rock, carbonatite, and fluorite–barite–bastnaesite ore conflict with the aforementioned genetic model. It should be noted that carbonatite, phlogopite–calcite–albite rock, and fluorite–barite–bastnaesite ore proper were formed from mineral-forming media differing in chemical composition and corresponding to distinct steps in the evolution of the most likely common volcanic–plutonic system. This follows from the fact that all rocks and ore, being located in the same tectonic structural unit, nevertheless occur as isolated geological bodies distinct in bulk chemical composition. The mechanism operating in the evolving volcanic–plutonic system was apparently related to multistage separation of immiscible liquids. This phenomenon, documented by the study of mineral-forming media, is crucial for the formation of many alkaline carbonatite-bearing rock complexes, when the primary carbonate-silicate melt separates into silicate and carbonate liquids. In turn, the carbonate melt was differentiated into carbonate, alkali sulfate, and alkali chloride melts (Panina and Motorina, 2008). It is evident that additional studies of mineral-forming media inclusions from all rock varieties, especially phonolite and carbonatite, are needed to provide insights into the formation mechanism of the Kizilcaören rock complex.

Genetic Type of the Kizilcaören Deposit

Summing up the above reasoning, we emphasize once again that the fluorite–barite–bastnaesite ore at the Kizilcaören deposit is closely associated with carbonate–feldspathic rocks, carbonatites, and subvolcanic phonolite. Examples of similar rock associations elsewhere in the world are not numerous.

Mineralization closest in phase composition is known at the Gallinas Mountains fluorite–bastnaesite deposit in the United States (Perhac and Heinrich, 1964; Williams-Jones et al., 2000). Skarn, veins, explosion pipes, and breccia with iron, copper–REE–fluorite, and REE–fluorite mineralization were

formed here in association with trachyte, phonolite, and syenite. It has been suggested that carbonatite occurs at a deep level.

In southern Mongolia, the Mushugai-Khuduk, Bayan-Khushuu, and Khotgor volcanic–plutonic complexes consist of melanephelinite, shonkinite, alkali syenite, trachyte, and phonolite, as well as magmatic magnetite–apatite rock, carbonatite, and late fluorite–celestine rock with REE mineralization (Samoilov and Kovalenko, 1983; Andreev, 1995; Andreeva et al., 1998, 1999).

A series of carbonatite-bearing rock complexes, including the Arshan and Southern occurrences (Nikiforov et al., 2002; Doroshkevich et al., 2008) with REE mineralization were formed during the Late Mesozoic stage of magmatic activity in the West Transbaikal Rift Domain (Yarmolyuk and Ivanov, 2000).

The late Quaternary Khanashin (Khan Neshin) volcanic complex in Afghanistan is composed of the phonolite–carbonatite series. Carbonatites of this complex varying in composition contain barite, celestine, strontianite, fluorite, apatite, and REE minerals: bastnaesite, parisite, synchysite, carbocernaite, and khanneshite. The total $LREE_2O_3$ content exceeds 3 wt % (Tucker et al., 2012). Similar volcanic associations are known in East Africa, e.g., the Nkombwa and Kangankunde complexes (Woolley, 2001).

Similar orebody structure and partly the same mineralization are characteristic of carbonatites in the Central Tuva area (Nikiforov et al., 2005, 2006; Bolonin et al., 2009). The Au-bearing copper–base-metal sulfide, fluorite–barite–REE, and U–Th occurrences in the Taimyr volcanic–plutonic complex (Proskurin et al., 2010) are apparently related to similar association.

The above examples show that the considered rock associations are formed under hypabyssal conditions and related to within-plate magmatism that develops in consolidated crustal blocks of young and ancient platforms. They are characterized by similar geochemical specialization (F, S, CO_2, Sr, Ba, LREE) and a similar set of rocks, which include alkaline and subalkaline silicate intermediate rocks (trachyte, phonolite, alkali syenite), solidified melted salts (carbonatite, apatite–magnetite, and other rocks), and various types of related postmagmatic (hydrothermal) mineralization. The aforementioned ore objects are distinguished only by volumetric proportions and specific mineralogical types of silicate and salt igneous rocks and their hydrothermal derivatives. The Kizilcaören fluorite–barite–REE deposit is one of possible combinations of these rock groups and correspondingly one of variants of ore-forming medium evolution, which results in accumulation of ore components.

CONCLUSIONS

(1) The fluorite–barite–REE ore of the Kizilcaören deposit, western Anatolia, Turkey is an constituent of the subvolcanic complex, which combines (from earlier to later): (1) phonolite and trachyte stocks; (2) carbonatite and carbonate–silicate dikelike bodies; and (3) fluorite–barite–bastnaesite ore, which forms thick and homogeneous veins and cements brecciated rocks.

(2) According to the results of K–Ar isotope datings, phonolite, phlogopite–calcite–albite rock, and carbonatite were formed 25–24 Ma ago during the Chattian Age. The ore is younger than the above-listed igneous rocks.

(3) Nepheline, clinopyroxene (diopside–augite–aegirine), K–Na feldspar, analcime, apatite, and a mineral from the eudialyte group are the primary mineral phases of phonolite. Hauyne, analcime, and zeolite (Ca-thomsonite?) have been identified as pseudomorphs after nepheline. Zeolite microveinlets are noted as well.

(4) Carbonatite is composed primarily of calcite; Fe–Mg mica, apatite, parisite, pyrochlore, barite, and pyrite were also identified. Phlogopite–calcite–albite rock allied to carbonatite contains Fe–Mg mica, apatite, zircon, barite, and pyrite. Supergene Fe and Mn hydroxides with Pb and Ba admixtures are noteworthy.

(5) The ore is an inequigranular aggregate of fluorite, barite, and Th-bearing Ca-bastnaesite. Fe–Mg mica, K-feldspar, Nb-bearing rutile, and pyrochlore occur in accessory amounts. The primary fluorite–barite–bastnaesite ore underwent deep alteration under supergene conditions, which, in particular, gave rise to leaching of presumably Ca–Mn–Fe carbonates and cementation of the residual bastnaesite–barite–fluorite framework by Fe and Mn hydroxides.

ACKNOWLEDGMENTS

We thank A.V. Bolonin and P.M. Kartashov for their consultations and constructive criticism, and we deeply appreciate the comprehensive reviews by A.A. Nosova and I.V. Vikent'ev.

REFERENCES

Altuncu, S., Comparative investigation of fluoride deposits in Turkey, *Ph.D. Thesis*, Istanbul: Istanbul Univesity, 2009.

Andreev, G.V., Geology and mineralogy of ore at the Apatitovoe deposit, the Mushugai ore cluster, Mongolia, *Otech. Geol.*, 1995, no. 10, pp. 39–44.

Andreeva, I.A., Naumov, V.B., Kovalenko, V.I., and Kononkova, N.N., Fluoride–sulfate and chloride–sulfate salt melts of the carbonatite-bearing complex Mushugai Khuduk, southern Mongolia, *Petrology*, 1998, vol. 6, no. 3, pp. 284–292.

Andreeva, I.A., Naumov, V.B., Kovalenko, V.I., and Kononkova, N.N., The magma composition and genesis of theralite from the Mushugai Khuduk carbonatite-bearing

complex in southern Mongolia, *Geochem. Int.*, 1999, vol. 37, no. 8, pp. 735–749.

Bolonin, A.V., Nikiforov, A.V., Lykhin, D.A., and Sugorakova, A.M., The Chailag-Khem fluorite-barium-strontium rare earth carbonatite occurrence, the Western Sayan Range, Russia, *Geol. Ore Deposits*, 2009, vol. 51, no. 1, pp. 17–32.

Borodin, L.S. and Nazarenko, I.I., Chemical composition of pyrochlore and isomorp[hic replacements in $A_2B_2X_7$ molecule, *Geokhimiya*, 1957, no. 4, pp. 278–295.

Delaloye, M. and Özgenç, I., Petrography and age determinations of the alkaline volcanic rocks and carbonatite of Kızılcaören district, Beylikahır-Eskişehir, Turkey, *Schweiz. Min. Petrogr.*, 1983, vol. 63, pp. 289–294.

Dilek, Y. and Altunkaynak, S., Geochemical and temporal evolution of Cenozoic magmatism in western Turkey: mantle response to collision, slab break-off, and lithospheric tearing in an orogenic belt, *Geol. Soc. London Spec. Publ.*, 2009, vol. 311, pp. 631–655.

Dilek, Y. and Altunkaynak, S., Geochemistry of Neogene–Quaternary alkaline volcanism in western Anatolia, Turkey, and implications for the Aegean mantle, *Int. Geol. Rev.*, 2010, vol. 52, pp. 631–655.

Doroshkevich, A.G., Ripp, G.S., Viladkar, S.G., and Vladykin, N.V., The Arshan REE carbonatites, southwestern Transbaikalia: mineralogy, paragenesis, and evolution, *Can. Mineral.*, 2008, vol. 46, pp. 807–823.

Gültekin A.H., Örgün Y., and Suner, F., Geology, mineralogy and fluid inclusion data of the Kizilcaören fluorite–barite–REE deposit, Eskisehir, Turkey, *J. Asian Earth Sci.*, 2003, vol. 21, pp. 365–376.

Hatzl, T. and Morteani, G., The hydrothermal formation of bastnaesite and fluocerite by decarbonatization of calciocarbonatites at high HF-fugacity at Kizilçaören (Turkey), in *Rare Earth Minerals: Chemistry, Origin and Ore deposits*, London: Natural History Museum, 1993, pp. 47–49.

Moix, P. and Beccaletto, L., Kozur H. W. et al., A new classification of the Turkish terranes and sutures and its implication for the paleotectonic history of the region, *Tectonophysics*, 2008, vol. 451, pp. 7–39.

Nikiforov, A.V., Bolonin, A.V., Sugorakova, A.M., et al., Carbonatites of central Tuva: Geological structure and mineral and chemical composition, *Geol. Ore Deposits*, 2005, vol. 47, no. 4, pp. 326–345.

Nikiforov, A.V., Bolonin, A.V., Pokrovsky, B.G., et al., Isotope geochemistry (O, C, S, Sr) and Rb–Sr age of carbonatites in central Tuva, *Geol. Ore Deposits*, 2006, vol. 48, no. 4, pp. 256–276.

Okay, A.I., Harris, N.B.W., and Kelley, S.P., Exhumation of blueschists along a Tethyan suture in Northwest Turkey, *Tectonophysics*, 1998, vol. 285, pp. 275–299.

Nikiforov, A.V., Yarmolyuk, V.V., Kovalenko, V.I., et al., Late Mesozoic carbonatites of western Transbaikalia: Isotopic–geochemical characteristics and sources, *Petrology,* 2002, vol. 10, no. 2, pp. 146–164.

Özgenç I., Geology and REE-geochemistry of carbothermal bastnaesite–fluorite–barite deposit of Kızılcaören (Sivrihisar, Eskişehir), *Geol. Bull. Turkey*, 1993, vol. 36, pp. 1–11.

Panina, L.I. and Motorina, I.V., Liquid immiscibility in deep-seated magmas and the generation of carbonatite melts, *Geochem. Int.*, 2008, vol. 46, no. 5, pp. 448–464.

Perhac, R.M. and Heinrich, E.W., Fluorite–bastnaesite deposits of the Gallinas Mountains, New Mexico and bastnaesite paragenesis, *Econ. Geol.*, 1964, vol. 59, pp. 226–239.

Proskurnin, V.F., Petrov, O.V., Gavrish, A.V., et al., Early Mesozoic carbonatite belt in Taimyr Peninsula, Litosfera, 2010, no. 3, pp. 95–102.

Samoilov, V.S. and Kovalenko, V.I., *Kompleksy shchelochnykh porod i karbonatitov Mongolii* (Complexes of Alkaline Rocks and Carbonatites in Mongolia), Moscow: Nauka, 1983.

Santfakıoğlu, E., Özen, H., and Hall, C., Petrogenesis of extension-related alkaline volcanism in Karaburhan (Sivrihisar–Eskisehir), NW Anatolia, Turkey, *J. Asian Earth Sci.*, 2009, vol. 35, pp. 502–515.

Sherlock, S., Kelley, S.P., Inger, S., Harris, N., and Okay, A.I., ^{40}Ar-^{39}Ar and Rb–Sr geochronology of high-pressure metamorphism and exhumation history of the Tavşanli Zone, NW Turkey, *Contrib. Mineral. Petrol.*, 1999, vol. 137, pp. 46–58.

Steiger, R.H. and Jager, E., Subcomission on Geochronology: Convention on the use of decay constants in geo- and cosmochronology, *Earth Planet. Sci. Lett.*, 1977, no. 36, pp. 359–362.

Stumpfl, E.F., Kırıkoğlu M.S. Fluorite–barite–rare earth deposit at Kızılcaören, Turkey, *Mitt. Osterr. Ges.*, 1986, vol. 78, pp. 193–200.

Tucker, R.D., Belkin, H.E., Schulz, K.J., et al., A major light rare-earth element (LREE) resource in the Khanneshin carbonatite complex, southern Afghanistan, *Econ. Geol.*, 2012, vol. 107, pp. 197–208.

Williams-Jones, A.E., Samson, I.M., and Olivo, G.R., The genesis of hydrothermal fluorite–REE deposits in the Gallinas Mountains, New Mexico, *Econ. Geol.*, 2000, vol. 95, no. 2, pp. 327–341.

Woolley, A.R., *Alkaline Rocks and Carbonatites of the World, Part 3: Africa*, London: Geol. Society London, 2001.

Yarmolyuk, V.V. and Ivanov, V.G., Late Mesozoic and Cenozoic magmatism and geodynamics of western Transbaikalia, *Geotectonics*, 2000, vol. 34, no. 2, pp. 121–140.

Translated by V. Popov

View publication stats